

**ENCLOSURE 12**

**WESTINGHOUSE WCAP-17085-NP, (NONPROPRIETARY) REVISION 1  
MONTICELLO REPLACEMENT STEAM DRYER STRUCTURAL EVALUATION FOR  
HIGH-CYCLE ACOUSTIC LOADS**

**119 pages follow**

Westinghouse Non-Proprietary Class 3

WCAP-17085-NP  
Revision 1

June 2010

# Monticello Replacement Steam Dryer Structural Evaluation for High-Cycle Acoustic Loads



**Westinghouse**

**WCAP-17085-NP**  
**Revision 1**

# **Monticello Replacement Steam Dryer Structural Evaluation for High-Cycle Acoustic Loads**

**Gianluca Longoni\***  
**Younus Munsi\***  
**Gary Plonczak\***  
**Richard Smith\***  
**David Suddaby\***  
**Robert Theuret\***  
**Leslie Wellstein\***

**Acoustic and Structural Analysis**

**June 2010**

Approved: David Forsyth\*, Manager  
Acoustic and Structural Analysis

\*Electronically approved records are authenticated in the electronic document management system.

---

Westinghouse Electric Company LLC  
P.O. Box 355  
Pittsburgh, PA 15230-0355

© 2010 Westinghouse Electric Company LLC  
All Rights Reserved

## Table of Contents

1	INTRODUCTION .....	1-1
2	METHODOLOGY .....	2-1
	2.1 OVERVIEW .....	2-1
	2.2 DESIGN REQUIREMENTS .....	2-1
	2.2.1 Endurance Strength Limits .....	2-1
	2.2.2 Young's Modulus Correction.....	2-1
	2.2.3 Fatigue Strength Reduction Factors.....	2-2
	2.3 DRYER GEOMETRY .....	2-2
3	FINITE ELEMENT MODEL DESCRIPTION .....	3-1
	3.1 STEAM DRYER GEOMETRY.....	3-1
	3.2 FINITE ELEMENT MODEL MESH AND CONNECTIVITY .....	3-2
	3.2.1 Vane-Bank Representation.....	3-2
	3.2.2 Lifting Rod Representation.....	3-3
	3.2.3 Dryer Skirt Submerged in Water.....	3-3
4	MATERIAL PROPERTIES .....	4-1
	4.1 STRUCTURAL DAMPING.....	4-1
5	MODAL ANALYSIS.....	5-1
6	LOAD APPLICATION.....	6-1
7	STRUCTURAL ANALYSIS .....	7-1
	7.1 HARMONIC ANALYSIS.....	7-1
	7.1.1 Unit Load Harmonic Solutions .....	7-1
	7.1.2 Overview – Time-History Solution.....	7-2
	7.1.3 Inverse Fourier Transform .....	7-3
	7.1.4 Frequency Scaling (Shifting).....	7-3
	7.2 POST-PROCESSING .....	7-4
	7.2.1 Primary Stress Evaluation.....	7-4
	7.2.2 Alternating Stress.....	7-4
	7.3 CALCULATION AND EVALUATION OF WELD STRESSES.....	7-5
	7.4 SUBMODELING TECHNIQUES .....	7-6
	7.5 [ ..... ] <sup>a,c</sup> .....	7-7
8	ANALYSIS RESULTS .....	8-1
	8.1 GLOBAL MODEL .....	8-1
	8.2 SUBMODELING .....	8-1

8.2.1 [ ]<sup>a,c</sup> ..... 8-1

8.2.2 [ ]<sup>a,c</sup> ..... 8-2

8.3 [ ]<sup>a,c</sup> ..... 8-2

9 SUMMARY OF RESULTS AND CONCLUSIONS ..... 9-1

10 REFERENCES ..... 10-1

---

**LIST OF TABLES**

Table 4-1	Summary of Material Properties .....	4-2
Table 8-1	Maximum of [ ] <sup>a,c</sup> for EPU Conditions .....	8-3
Table 8-2	Maximum of [ ] <sup>a,c</sup> for CLTP Conditions .....	8-5
Table 8-3	Summary of Results – [ ] <sup>a,c</sup> – CLTP Conditions.....	8-7
Table 8-4	Summary of Results – [ ] <sup>a,c</sup> – EPU Conditions .....	8-8
Table 8-5	Summary of Results – [ ] <sup>a,c</sup> – CLTP Conditions.....	8-9
Table 8-6	Summary of Results – [ ] <sup>a,c</sup> – EPU Conditions .....	8-10
Table 8-7	Summary of Results – [ ] <sup>a,c</sup> – CLTP Conditions.....	8-11
Table 8-8	Summary of Results – [ ] <sup>a,c</sup> – EPU Conditions .....	8-12
Table 9-1	Summary of Results: EPU Conditions.....	9-2
Table 9-2	Summary of Results: CLTP Conditions .....	9-3

## LIST OF FIGURES

Figure 1-1	Schematic of Monticello Replacement Steam Dryer.....	1-2
Figure 2-1	Geometry Plot: Overall Dryer.....	2-3
Figure 2-2	Geometry Plot: Cut-Away View .....	2-4
Figure 2-3	Geometry Plot: Dryer Hoods .....	2-5
Figure 2-4	Geometry Plot: Skirt and Drain Region.....	2-6
Figure 2-5	Geometry Plot: One-Eighth Sector .....	2-7
Figure 2-6	Geometry Plot: Dryer Vane-Bank Region .....	2-8
Figure 2-7	Geometry Plot: [ ..... ] <sup>a,c</sup> .....	2-9
Figure 2-8	Geometry Plot: [ ..... ] <sup>a,c</sup> .....	2-10
Figure 3-1	Overall Geometry of the Monticello Replacement Steam Dryer Model .....	3-4
Figure 3-2	Lower [ ..... ] <sup>a,c</sup> .....	3-5
Figure 3-3	Lower [ ..... ] <sup>a,c</sup> .....	3-6
Figure 3-4	Vane-Bank Structural Components.....	3-7
Figure 3-5	Vane-Bank Geometry.....	3-8
Figure 3-6	Dryer Hood Geometry .....	3-9
Figure 3-7	Skirt Geometry.....	3-10
Figure 3-8	[ ..... ] <sup>a,c</sup> .....	3-11
Figure 3-9	[ ..... ] <sup>a,c</sup> .....	3-12
Figure 3-10	[ ..... ] <sup>a,c</sup> .....	3-13
Figure 3-11	Lifting Lug Geometry.....	3-14
Figure 3-12	[ ..... ] <sup>a,c</sup> .....	3-15
Figure 3-13	[ ..... ] <sup>a,c</sup> .....	3-16
Figure 3-14	[ ..... ] <sup>a,c</sup> .....	3-17
Figure 3-15	[ ..... ] <sup>a,c</sup> .....	3-18
Figure 3-16	[ ..... ] <sup>a,c</sup> .....	3-19
Figure 3-17	Structural Components of Vane Bank.....	3-20
Figure 3-18	Non-Structural Components of Vane Bank.....	3-21
Figure 3-19	Vane-Bank Mass Blocks .....	3-22
Figure 3-20	Tie Rod Connection between Mass Blocks and End Plates.....	3-23
Figure 5-1	Modal Analysis: [ ..... ] <sup>a,c</sup> .....	5-2
Figure 5-2	Modal Analysis: [ ..... ] <sup>a,c</sup> .....	5-3

Figure 5-3	Modal Analysis: [ ] <sup>a,c</sup> .....	5-4
Figure 5-4	Modal Analysis: [ ] <sup>a,c</sup> .....	5-5
Figure 5-5	Modal Analysis: [ ] <sup>a,c</sup> .....	5-6
Figure 5-6	Modal Analysis: [ ] <sup>a,c</sup> .....	5-7
Figure 5-7	Modal Analysis: [ ] <sup>a,c</sup> .....	5-8
Figure 5-8	Modal Analysis: [ ] <sup>a,c</sup> .....	5-9
Figure 6-1	Helmholtz Acoustic Model .....	6-3
Figure 6-2	Three-Dimensional Views of the Acoustic Model .....	6-4
Figure 6-3	ACM and FEM Global Coordinate System Layout, Top View .....	6-5
Figure 6-4	ACM and FEM Global Coordinate System Layout, Section View .....	6-6
Figure 6-5	Applied Nodal Forces Due to Unit 60 Hz Load from Main Steam Line-A .....	6-7
Figure 6-6	Applied Nodal Forces Due to Unit 94.5 Hz Load from Main Steam Line-D .....	6-8
Figure 7-1	[ ] <sup>a,c</sup> .....	7-8
Figure 8-1	Effect of Frequency Shift on Stress Intensity: [ ] <sup>a,c</sup> EPU Operating Conditions .....	8-13
Figure 8-2	Effect of Frequency Shift on Stress Intensity: [ ] <sup>a,c</sup> EPU Operating Conditions .....	8-14
Figure 8-3	Stress Intensity Comparison between EPU and CLTP Conditions .....	8-15
Figure 8-4	EPU Stress Intensity Results: [ ] <sup>a,c</sup> .....	8-16
Figure 8-5	EPU Stress Intensity Results: [ ] <sup>a,c</sup> .....	8-17
Figure 8-6	EPU Stress Intensity Results: [ ] <sup>a,c</sup> .....	8-18
Figure 8-7	EPU Stress Intensity Results: [ ] <sup>a,c</sup> .....	8-19
Figure 8-8	EPU Stress Intensity Results: [ ] <sup>a,c</sup> .....	8-20
Figure 8-9	EPU Stress Intensity Results: [ ] <sup>a,c</sup> .....	8-21
Figure 8-10	EPU Stress Intensity Results: [ ] <sup>a,c</sup> .....	8-22
Figure 8-11	EPU Stress Intensity Results: [ ] <sup>a,c</sup> .....	8-23
Figure 8-12	Stress Intensity Results: [ ] <sup>a,c</sup> .....	8-24
Figure 8-13	[ ] <sup>a,c</sup> .....	8-25
Figure 8-14	[ ] <sup>a,c</sup> .....	8-26
Figure 8-15	[ ] <sup>a,c</sup> .....	8-27
Figure 8-16	[ ] <sup>a,c</sup> .....	8-28
Figure 8-17	[ ] <sup>a,c</sup> .....	8-29
Figure 8-18	[ ] <sup>a,c</sup> .....	8-30



Figure 8-19	[	] <sup>a,c</sup>	.....8-31
Figure 8-20	[	] <sup>a,c</sup>	.....8-32
Figure 8-21	[	] <sup>a,c</sup>	.....8-33
Figure 8-22	[	] <sup>a,c</sup>	.....8-34
Figure 8-23	[	] <sup>a,c</sup>	.....8-35

---

## Executive Summary

A high-cycle fatigue evaluation of the Westinghouse replacement steam dryer for the Monticello plant has been completed. Acoustic loads and stresses for both current licensed thermal power (CLTP) and extended power uprate (EPU) conditions have been evaluated for high-cycle fatigue and have been determined to meet the American Society of Mechanical Engineers (ASME) Boiler and Pressure Vessel (B&PV) Code Section III, Subsection NG criteria.

The results from these analyses indicate that for the Monticello replacement steam dryer at EPU operation, the smallest high-cycle fatigue stress ratio anywhere on the steam dryer is [ ]<sup>a,c</sup> and occurs on [ ]<sup>a,c</sup>. For CLTP conditions, a minimum stress ratio of [ ]<sup>a,c</sup> is calculated. These results account for all the end-to-end biases and uncertainties in the loads model and finite element analysis. To account for uncertainties in the modal frequency predictions of the finite element model (FEM), the stresses are also computed for loads that are shifted in the frequency domain by [ ]<sup>a,c</sup>.

---

**LIST OF ABBREVIATIONS**

<u>Abbreviation</u>	<u>Description</u>
ACM	acoustic circuit model
ASME	American Society of Mechanical Engineers
B&PV	boiler and pressure vessel
BWR	boiling water reactor
CLTP	currently licensed thermal power
EPU	extended power uprate
FEM	finite element model
FSRF	fatigue strength reduction factor
IFT	inverse Fourier transform
MSL	main steam line
3-D	three-dimensional

**Trademark Note:**

ANSYS, ANSYS Workbench, CFX, AUTODYN, and any and all ANSYS, Inc. product and service names are registered trademarks or trademarks of ANSYS, Inc. or its subsidiaries located in the United States or other countries.

---

## 1 INTRODUCTION

In 2002, after increasing power to 117% of the original licensed thermal power, the steam dryer in a boiling water reactor (BWR) experienced a series of structural failures. After extensive evaluation by various industry experts, the root cause of the dryer failures was determined to be acoustic fluctuating pressure loads on the dryer, resulting from resonances produced by steam flow in the main steam lines (MSLs) across safety and relief valve inlets. The failures experienced in the steam dryer of a BWR led to changes to Regulatory Guide 1.20, requiring plants to evaluate their steam dryer before any planned increase in power level.

The Monticello power plant has contracted Westinghouse for a replacement steam dryer, and is also planning a power uprate. In conjunction with the component replacement by Monticello and the planned power uprate, an analysis has been performed to qualify the replacement steam dryer, shown in Figure 1-1, for acoustic pressure loads. The process used to perform the analysis involves multiple acoustic and structural analyses, scale model testing, and several computer codes, both commercially available and special-purpose codes developed in conjunction with the evaluation of acoustic loads.

This report documents the qualification of the Monticello replacement steam dryer subject to acoustic loads. The extent of the qualification of the dryer that is addressed by the acoustic qualification is to assess the potential for high-cycle fatigue. Structural qualification of the replacement dryer for the remaining duty cycle of events applicable to the Monticello operating system is documented in Reference 1. Acoustic loads applicable to both CLTP and EPU conditions are evaluated. A dynamic analysis is performed using a harmonic load methodology.



**Figure 1-1 Schematic of Monticello Replacement Steam Dryer**

---

## 2 METHODOLOGY

### 2.1 OVERVIEW

An analysis has been performed to assess the structural integrity of the replacement dryer for the Monticello plant subject to acoustic loads. Acoustic loads applicable to both CLTP and EPU conditions are evaluated. Acoustic analyses are performed to determine the flow loads on the steam dryer. A dynamic analysis is performed using a harmonic load methodology that combines the use of a finite element representation of the dryer with special-purpose computer codes. The topics addressed in this report include acoustic load application, the dryer FEM, harmonic analysis, post-processing, stress results, and design margins for the Monticello replacement dryer.

### 2.2 DESIGN REQUIREMENTS

#### 2.2.1 Endurance Strength Limits

The replacement dryer is analyzed according to the 2004 Edition of the ASME B&PV Code, Subsection NG (Reference 2). This report documents the suitability of the replacement dryer for high-cycle fatigue loads resulting from acoustic loads. The governing criterion for the analysis is in terms of the allowable component fatigue usage. The objective of this analysis is to show that the maximum alternating stress intensity anywhere in the dryer is less than the material endurance strength at  $10^{11}$  cycles. The applicable fatigue curve for stainless steel (the dryer is manufactured from SS316L), is shown in Figure I-9.2.2 in Appendix I of the ASME Code. The evaluation of the replacement steam dryer for non-acoustic loads is documented in Reference 1.

[

] <sup>a,c</sup>.

As summarized in Section 8, [

] <sup>a,c</sup>.

[

] <sup>a,c</sup>.

#### 2.2.2 Young's Modulus Correction

Before comparing the maximum alternating stress intensity to the ASME Code endurance strength, it is necessary to account for the Young's modulus correction. The analysis uses a Young's modulus of

25.425 x 10<sup>6</sup> psi, compared to the value to construct the fatigue curves of 28.3 x 10<sup>6</sup> psi. The ratio that is applied to the calculated alternating stress intensities is 1.113 (28.3 / 25.425).

### **2.2.3 Fatigue Strength Reduction Factors**

When evaluating welds for fatigue, the calculated stress must be adjusted to account for fatigue strength reduction factors (FSRFs). Subsection NG of the ASME Code provides a table (Table NG-3352-1) summarizing appropriate FSRFs as a function of weld type and inspection techniques. Appropriate FSRFs have been established for each of the welds in the dryer, consistent with the weld type and inspection technique identified on the design drawings.

## **2.3 DRYER GEOMETRY**

Plots showing various aspects of the dryer configuration are provided in Figure 2-1 through Figure 2-8.

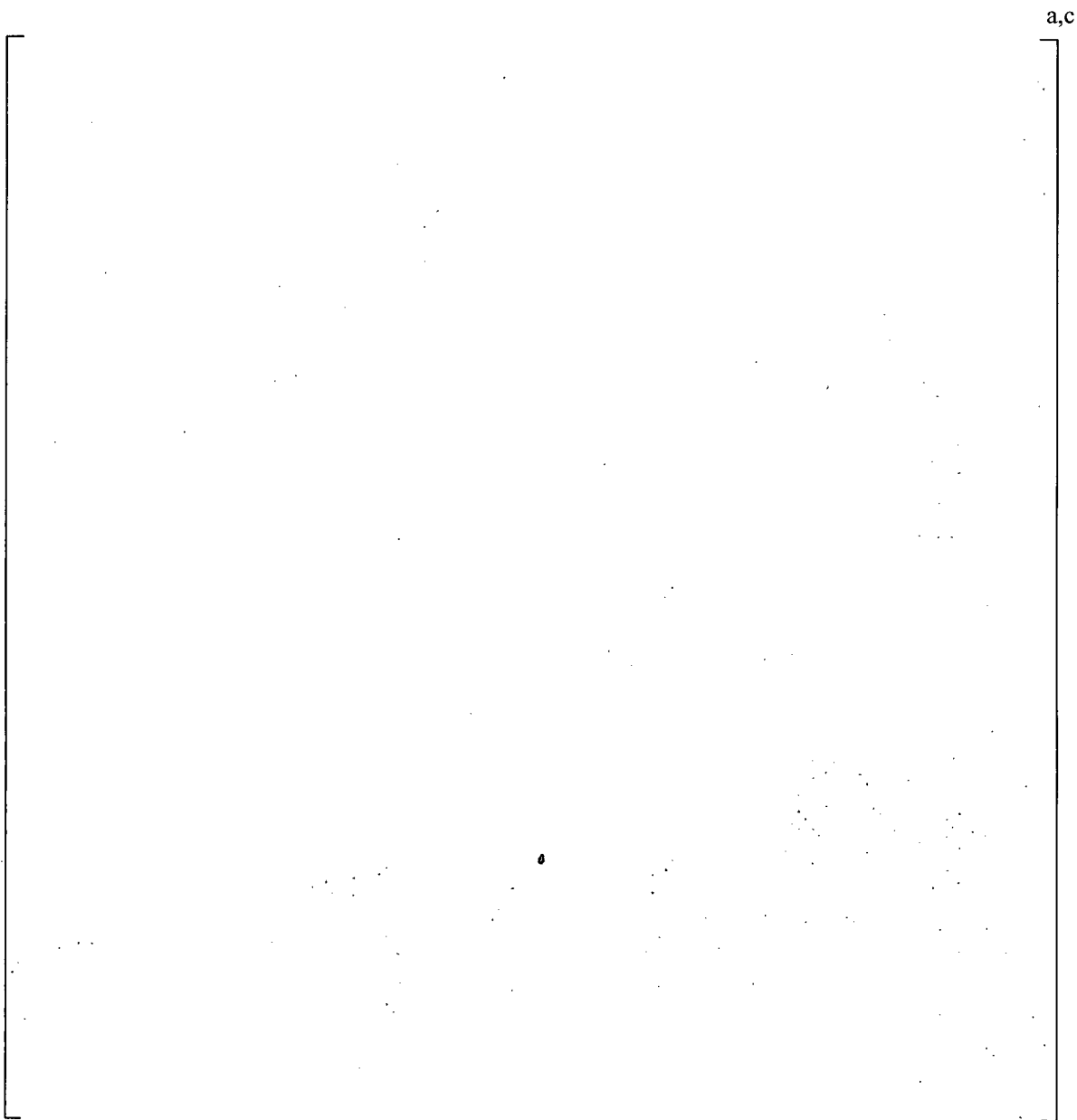


**Figure 2-1 Geometry Plot: Overall Dryer**



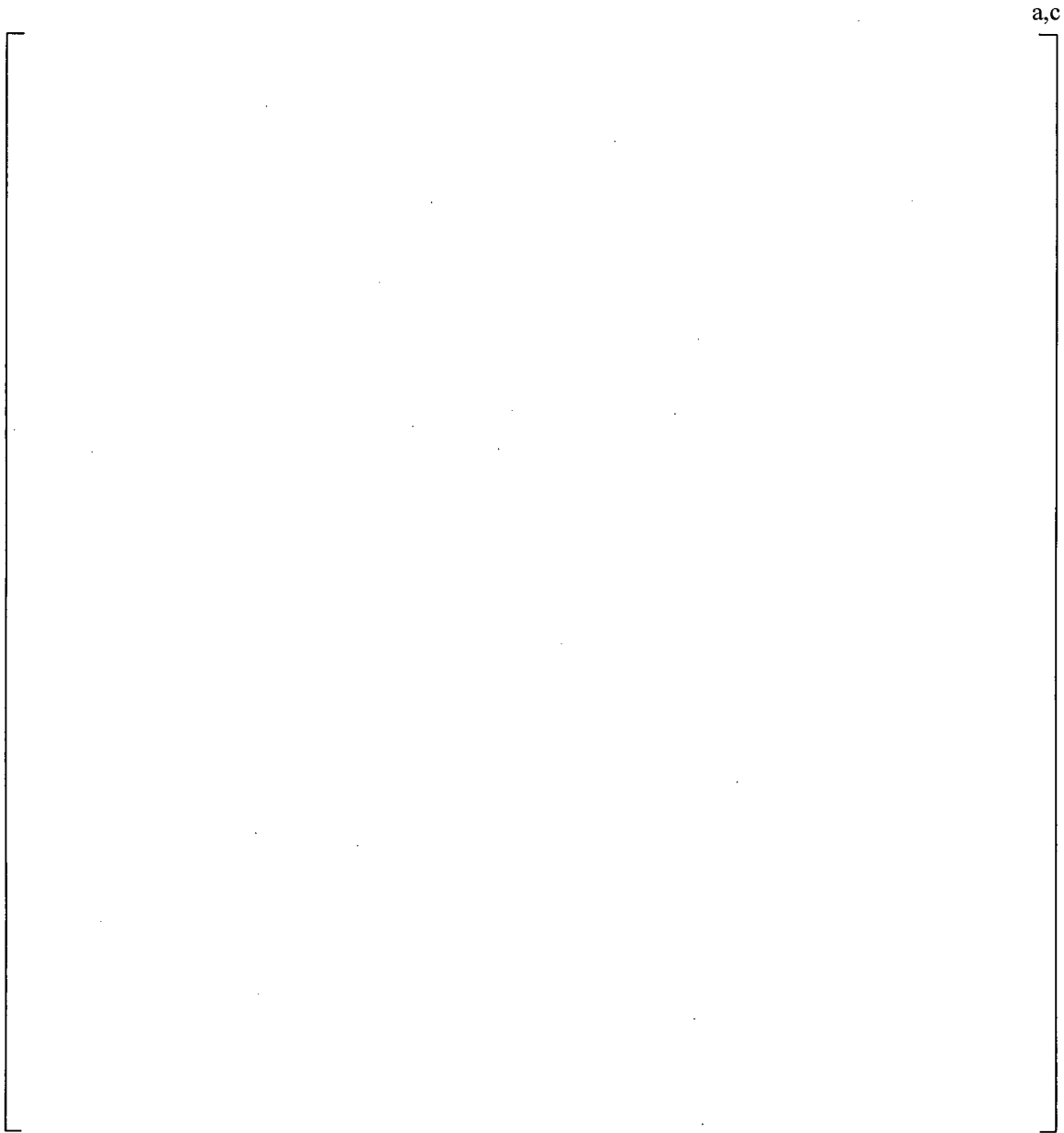


**Figure 2-2 Geometry Plot: Cut-Away View**

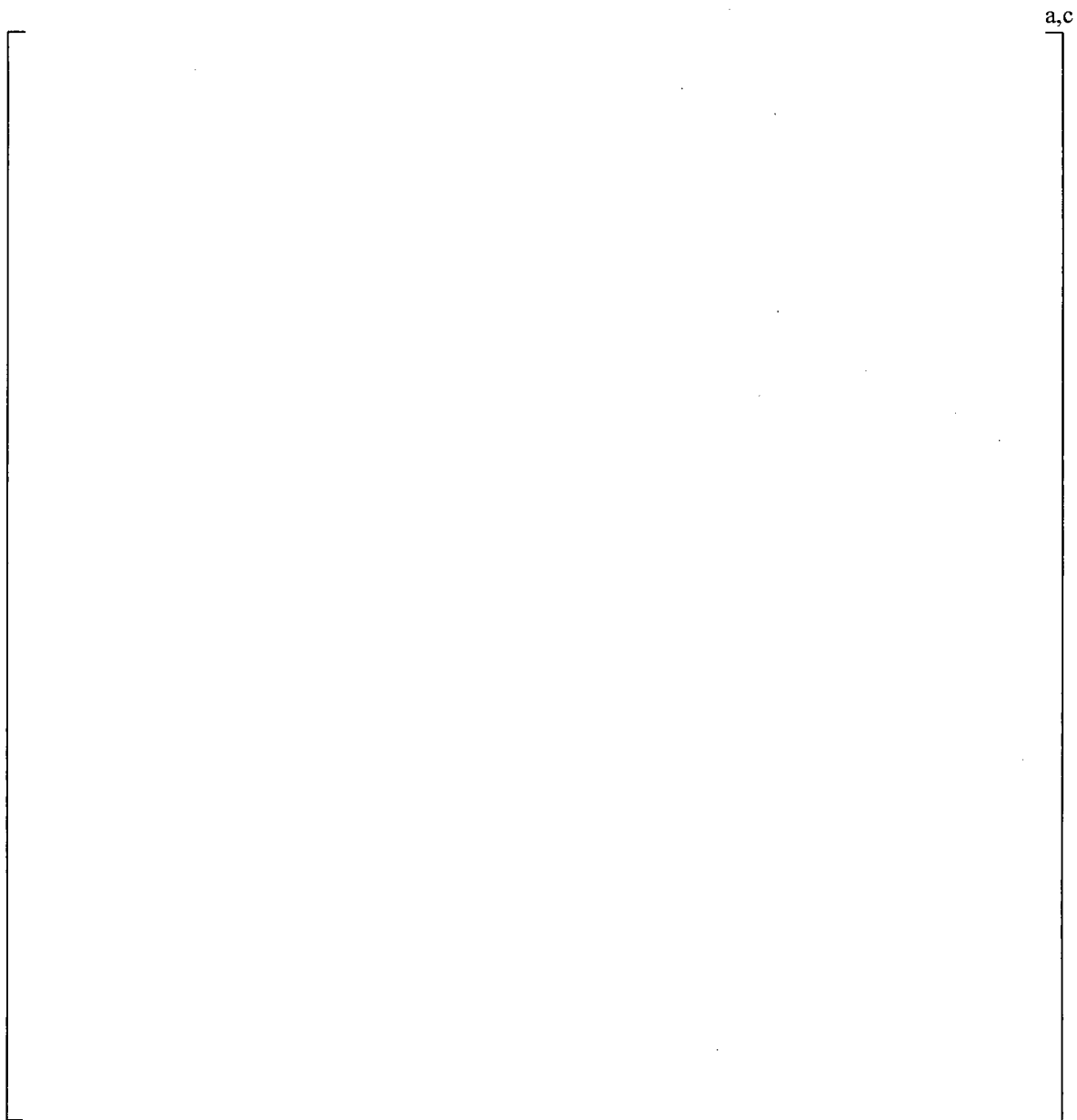


**Figure 2-3 Geometry Plot: Dryer Hoods**

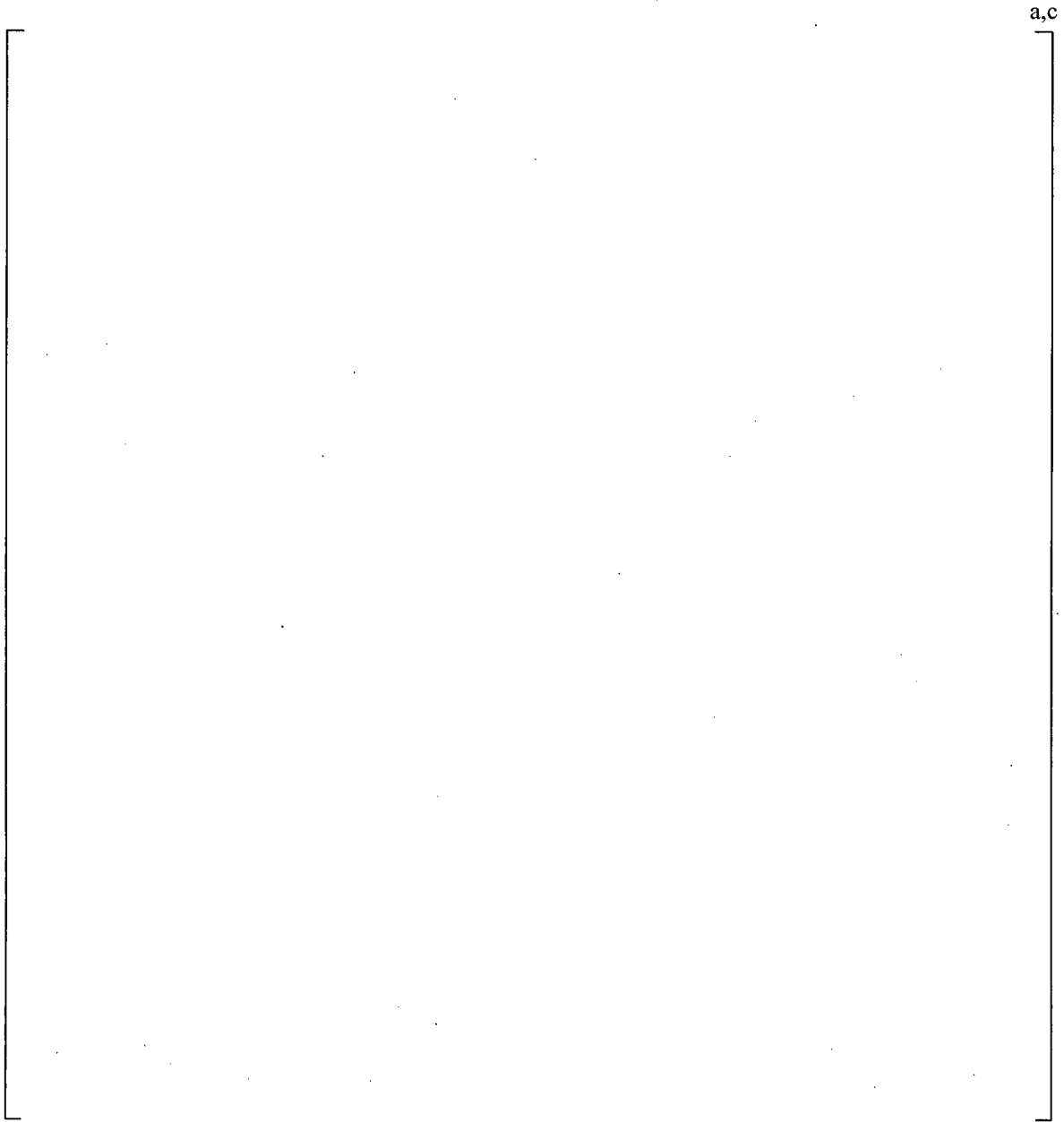


**Figure 2-4 Geometry Plot: Skirt and Drain Region**

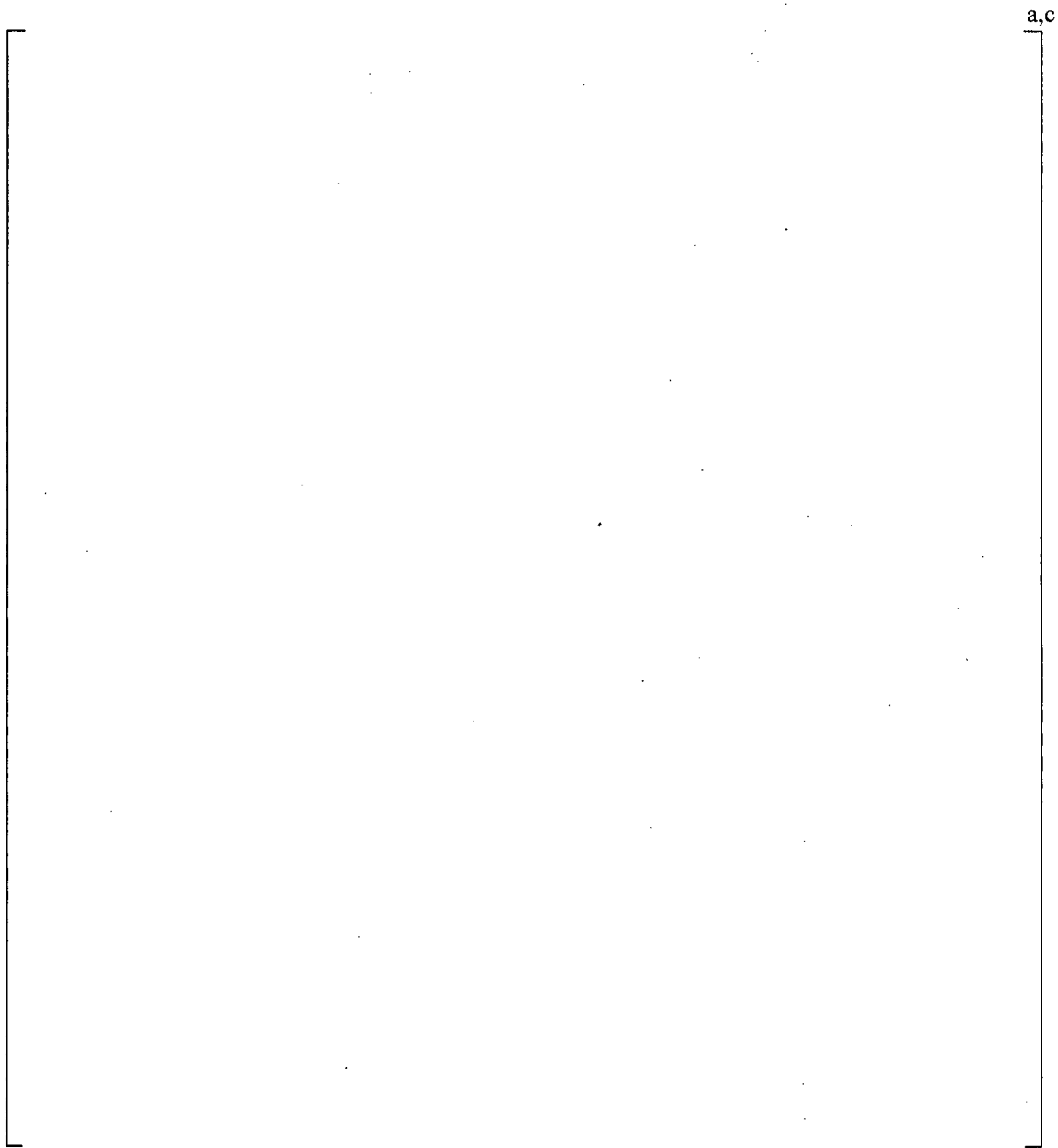


**Figure 2-5 Geometry Plot: One-Eighth Sector**

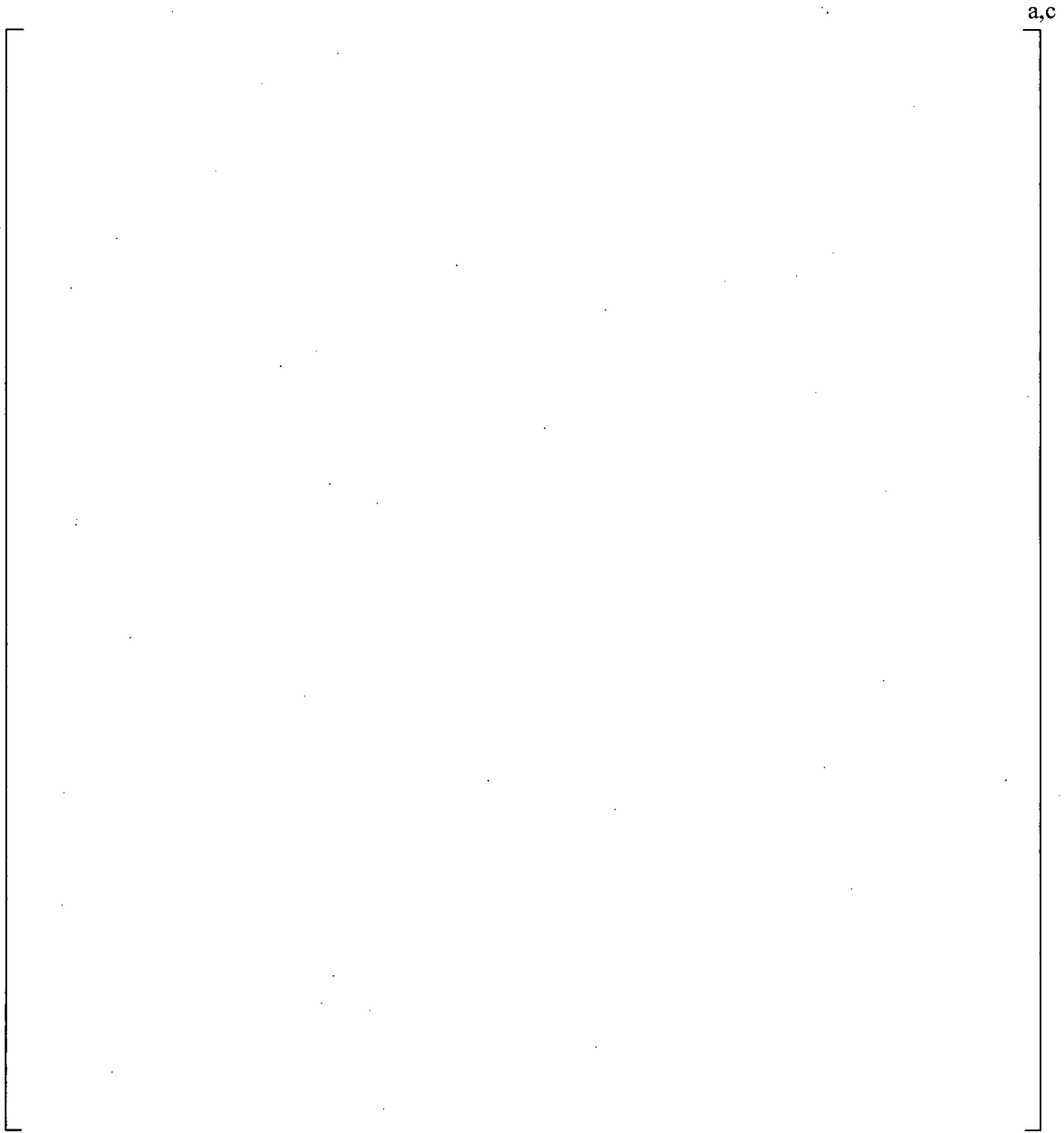


**Figure 2-6 Geometry Plot: Dryer Vane-Bank Region**

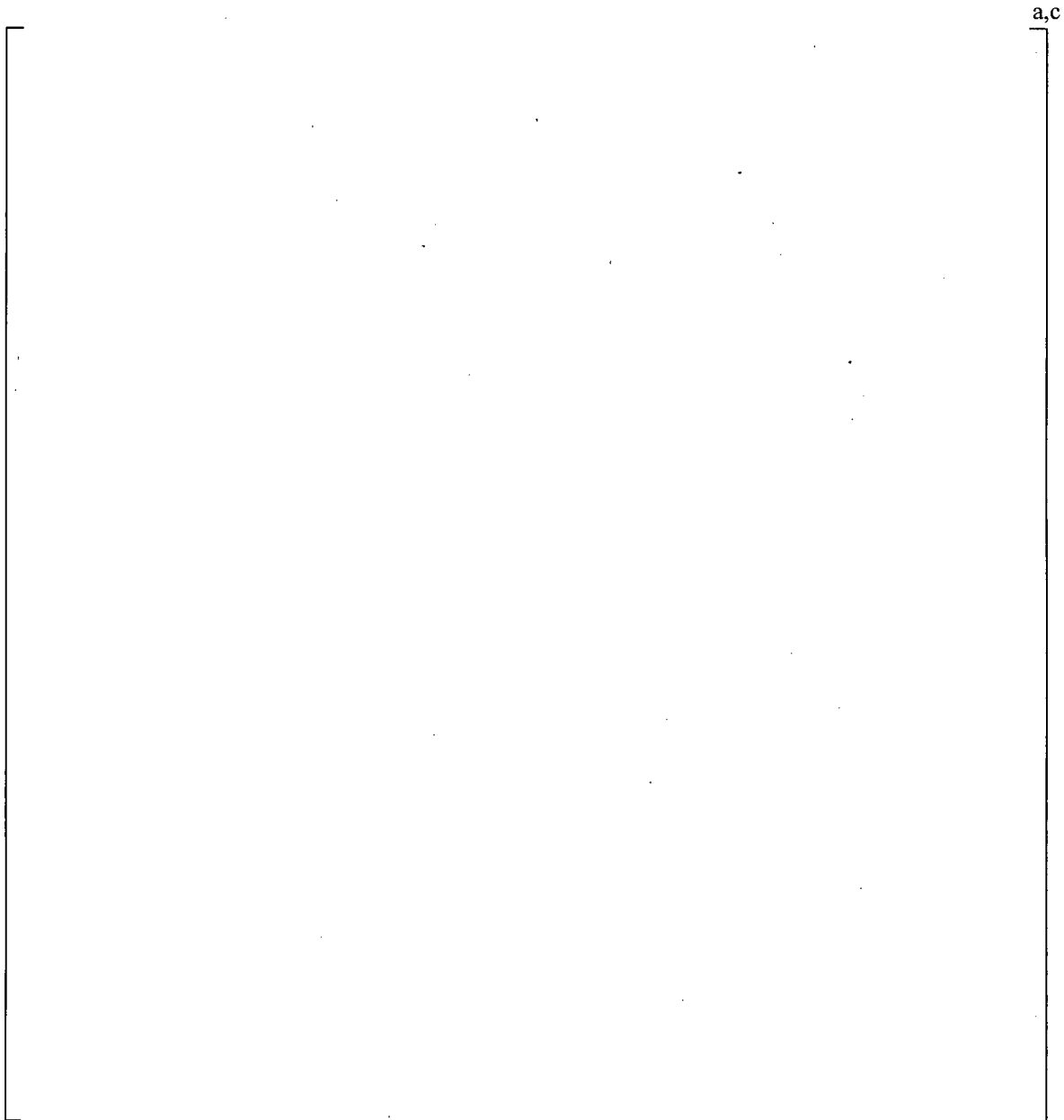
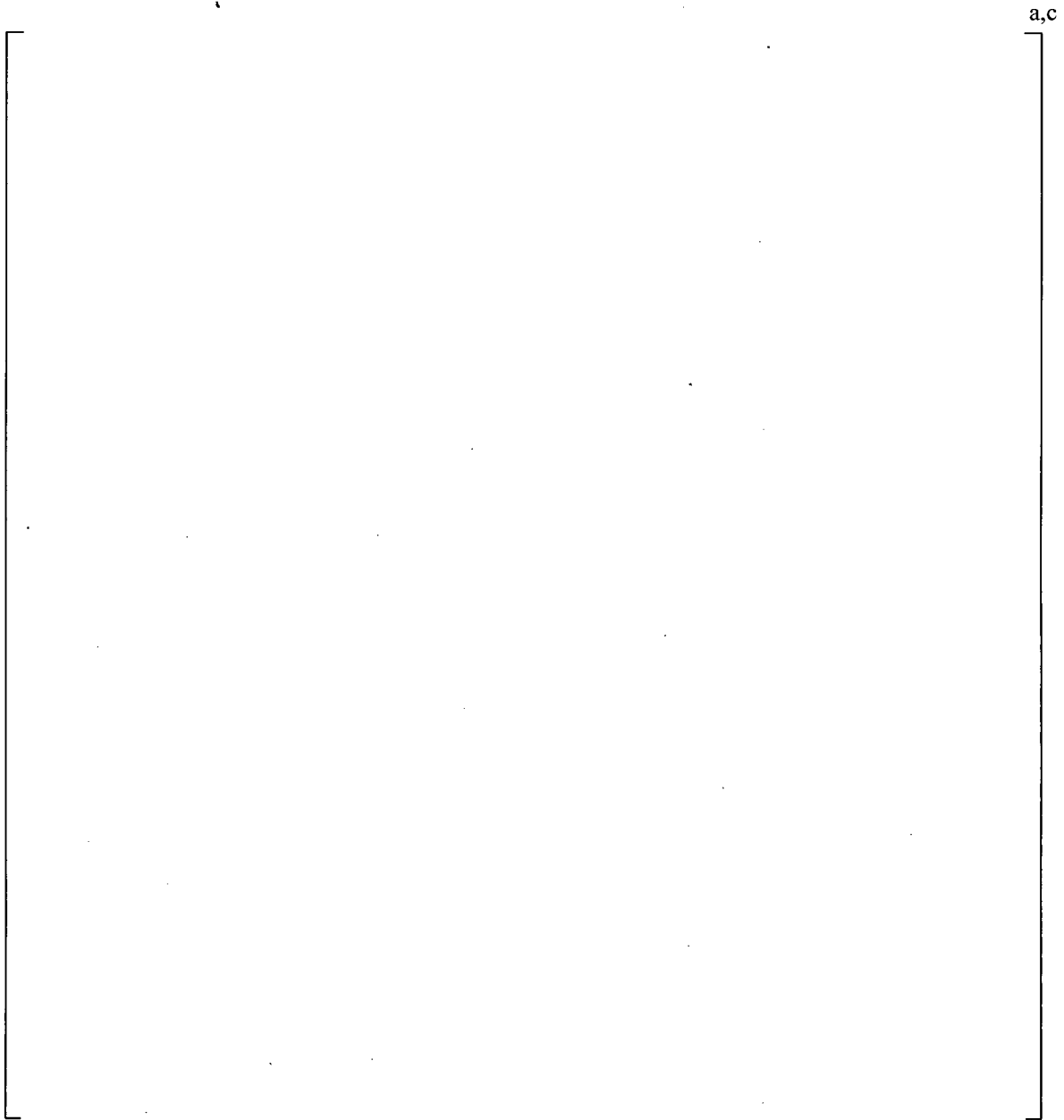


Figure 2-7 Geometry Plot: |<sup>a,c</sup>



**Figure 2-8 Geometry Plot:** [ ]<sup>a,c</sup>

### 3 FINITE ELEMENT MODEL DESCRIPTION

#### 3.1 STEAM DRYER GEOMETRY

The Monticello replacement steam dryer FEM, generated using the ANSYS® computer code<sup>1</sup>, is shown in Figure 3-1. The model consists primarily of [

]a,c.

[

]a,c.

The dryer structure includes [

]a,c.

The [

]a,c.

Figure 3-11 shows the lifting lug arrangement. Figure 3-12 and Figure 3-13 show details of the hood mesh. Note that the different colors in all of the figures represent different dryer components based on either plate thickness or function. These components can be selected for individual post processing.

---

<sup>1</sup> The analysis qualification of the Monticello replacement steam dryer was performed using the ANSYS computer code, Release 11, Service Pack 1.



### 3.2 FINITE ELEMENT MODEL MESH AND CONNECTIVITY

The dryer plates are all modeled [

] <sup>a,c</sup>.

The vane-bank [

] <sup>a,c</sup>.

[

] <sup>a,c</sup> are shown in Figure 3-16.

#### 3.2.1 Vane-Bank Representation

The vane-bank modules are box-like structures with many internal hanging chevrons. [

and are shown in more detail in Figure 3-17. ] <sup>a,c</sup>

The perforated plates [

] <sup>a,c</sup> are shown in Figure 3-18.

Also shown in Figure 3-18 are the [

] <sup>a,c</sup>.

The vane-bank [

] <sup>a,c</sup> are shown in Figure 3-14.

### 3.2.2 Lifting Rod Representation

The lifting rod is modeled [

] <sup>a,c</sup> are shown in Figure 3-16.

### 3.2.3 Dryer Skirt Submerged in Water

The dryer skirt is partially submerged in water. The skirt and drain channel components are separated into groups above and below the water line. The acoustic loading is only applied to elements above the water line. The material density for the stainless steel below water has been adjusted to account for the effect of the hydrodynamic mass.

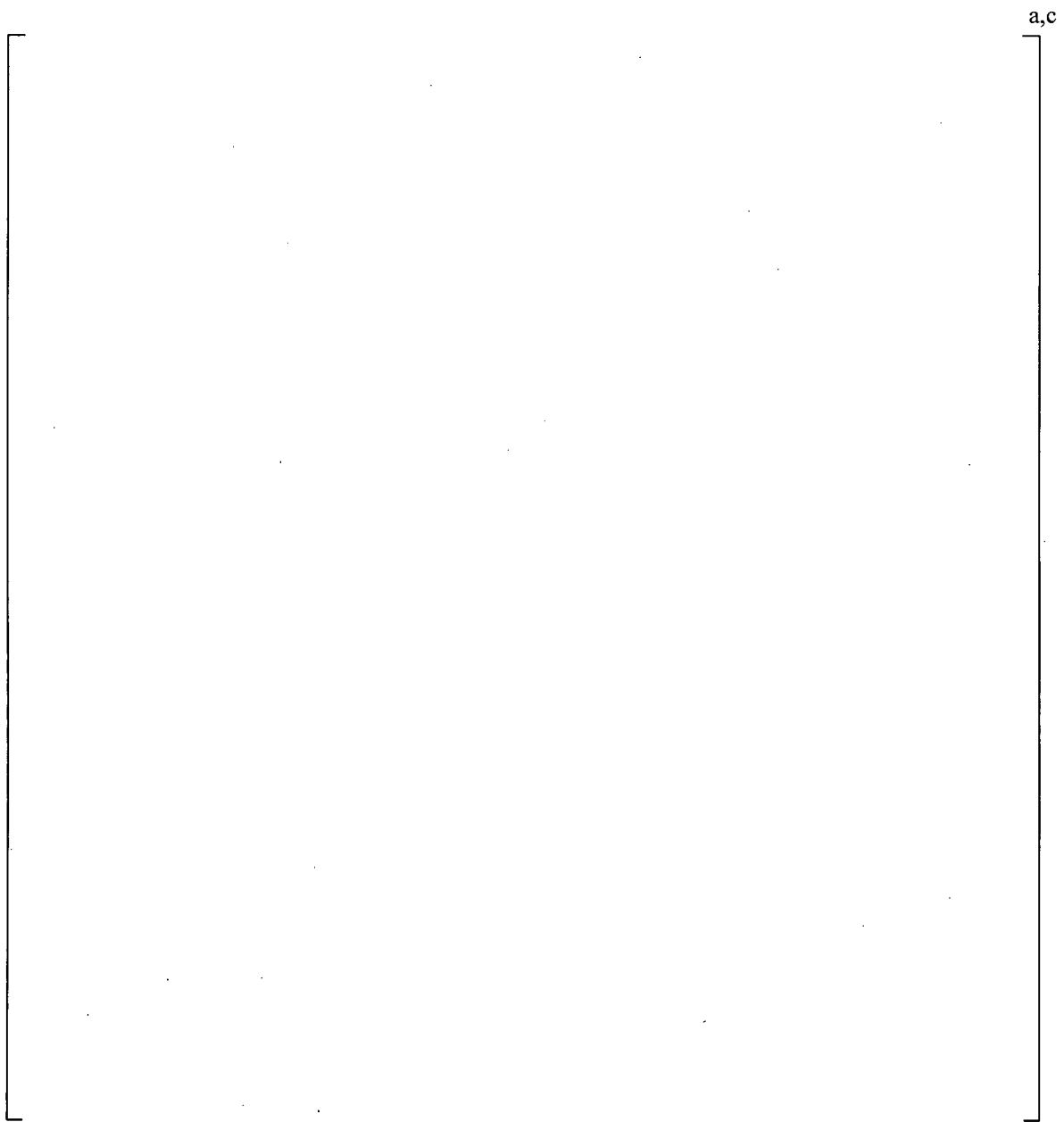


**Figure 3-1 Overall Geometry of the Monticello Replacement Steam Dryer Model**

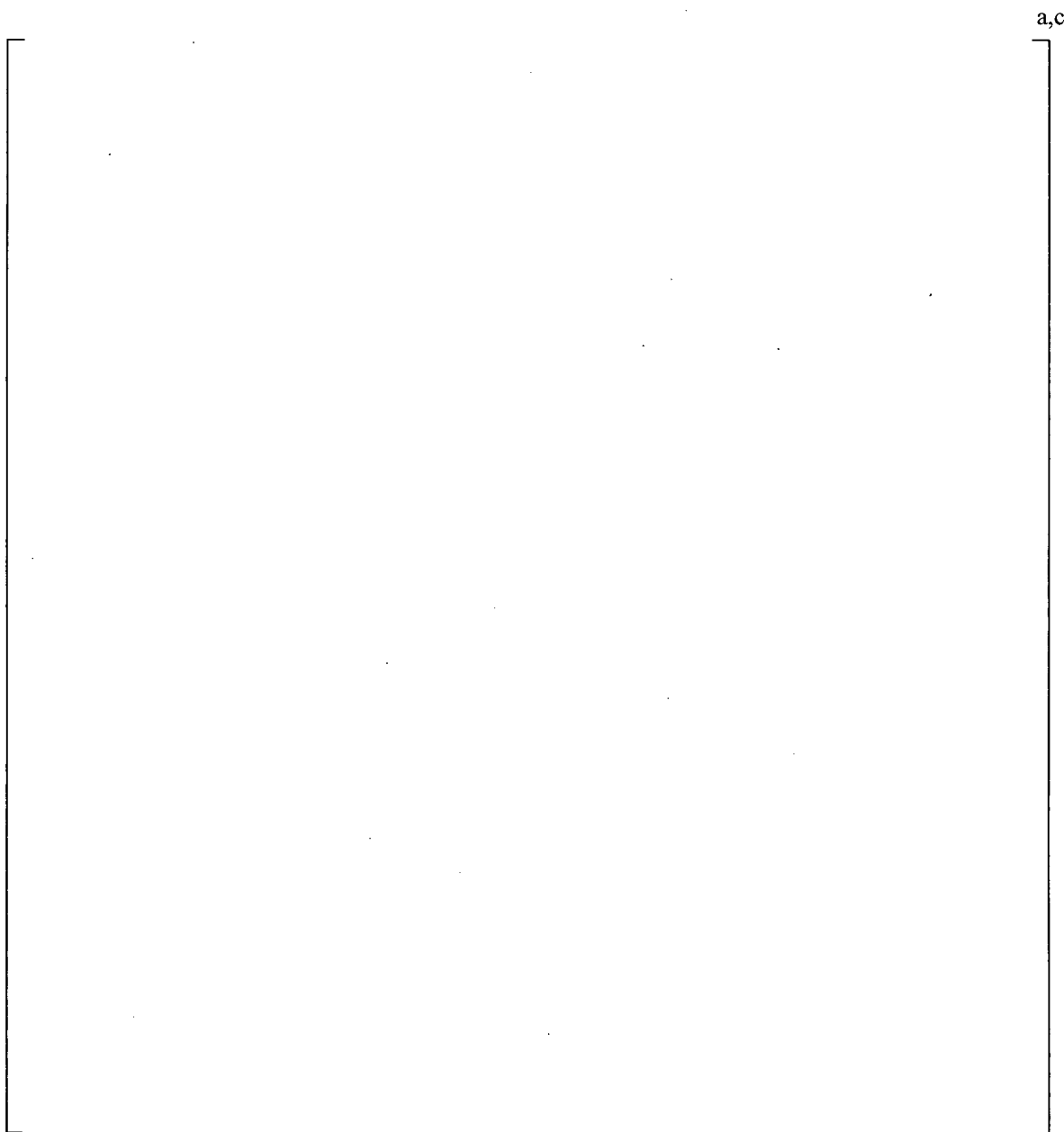
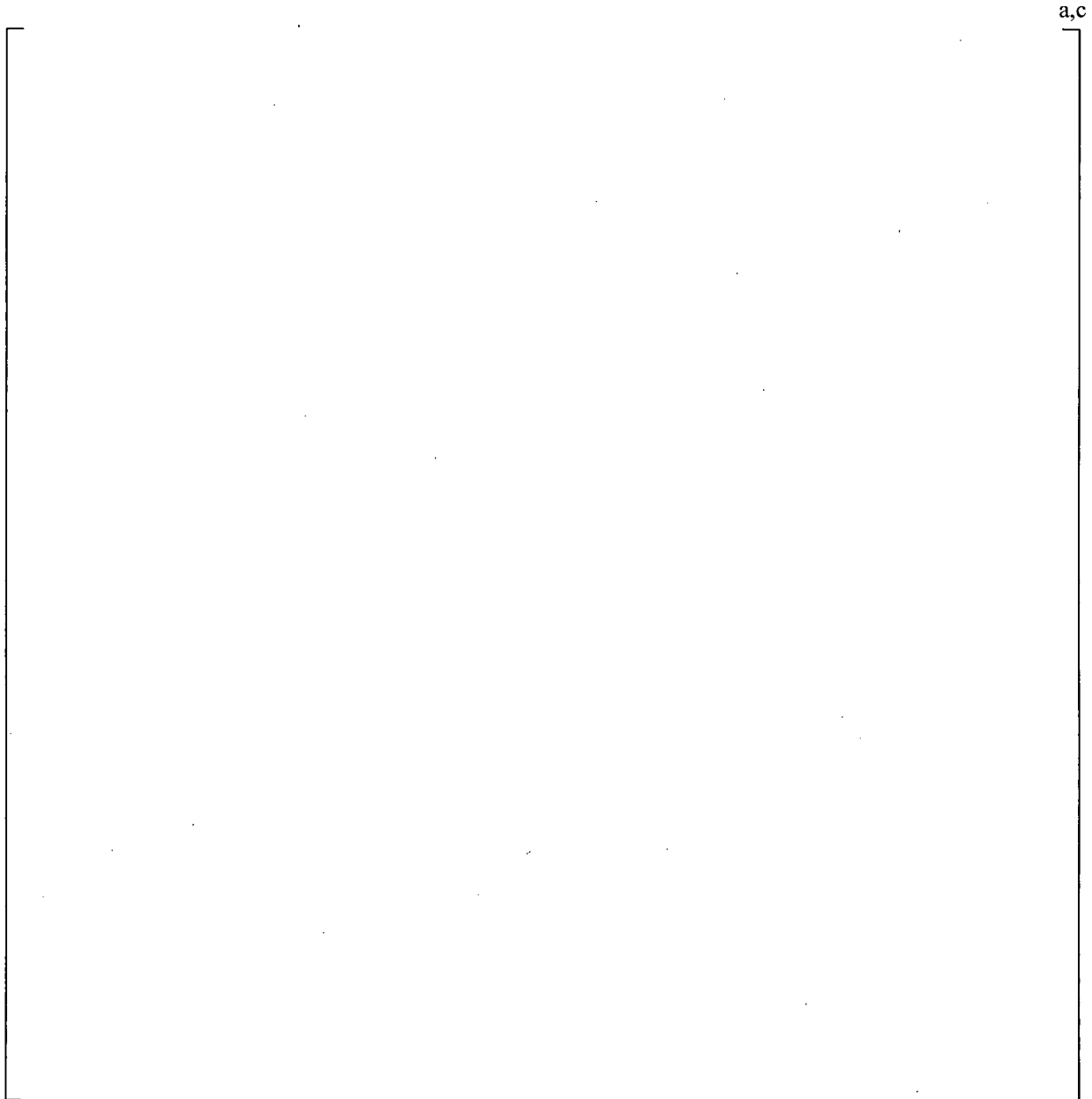
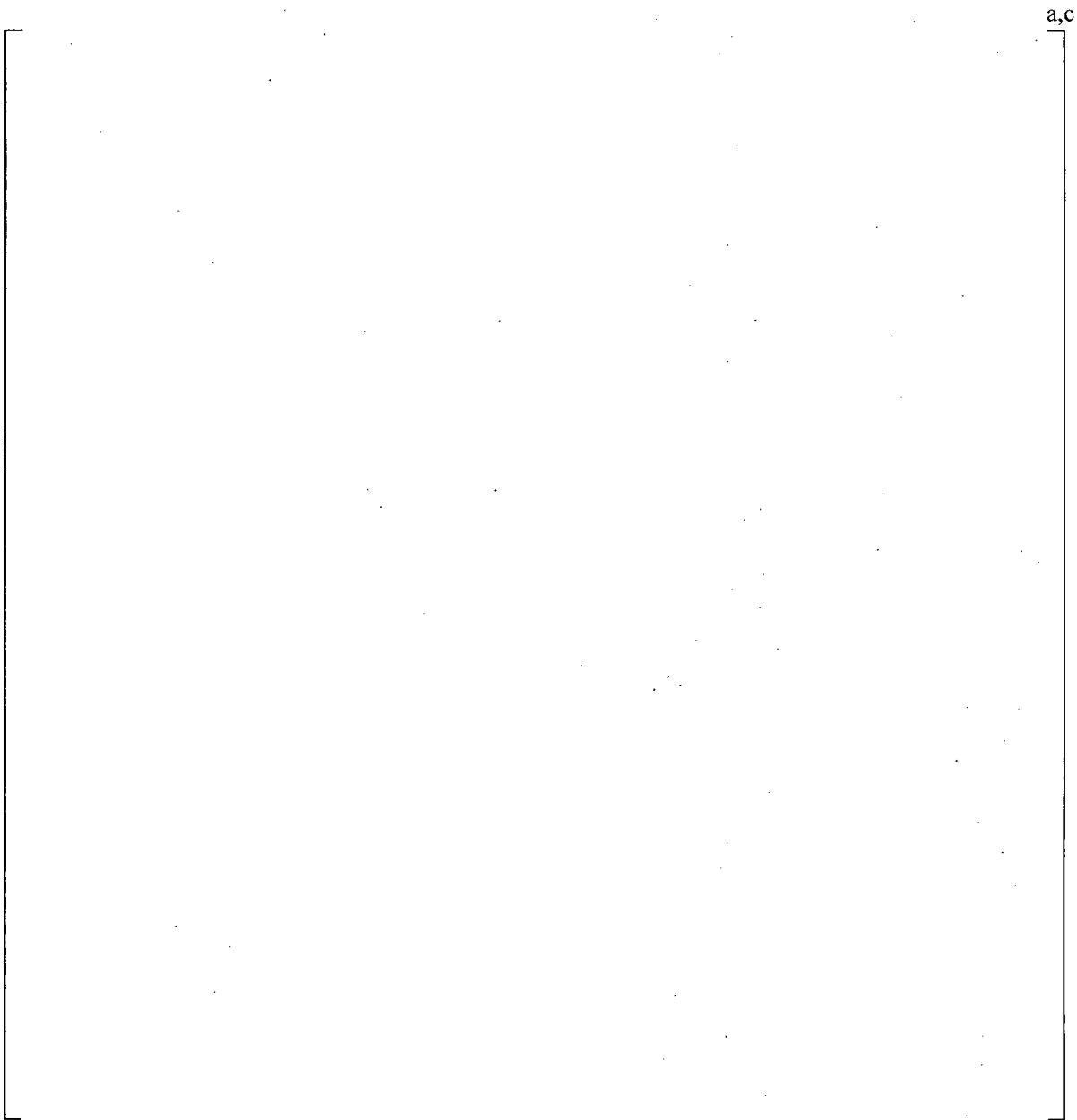


Figure 3-2 Lower | ]<sup>a,c</sup>



**Figure 3-3 Lower |**

**|<sup>a,c</sup>**



**Figure 3-4 Vane-Bank Structural Components**

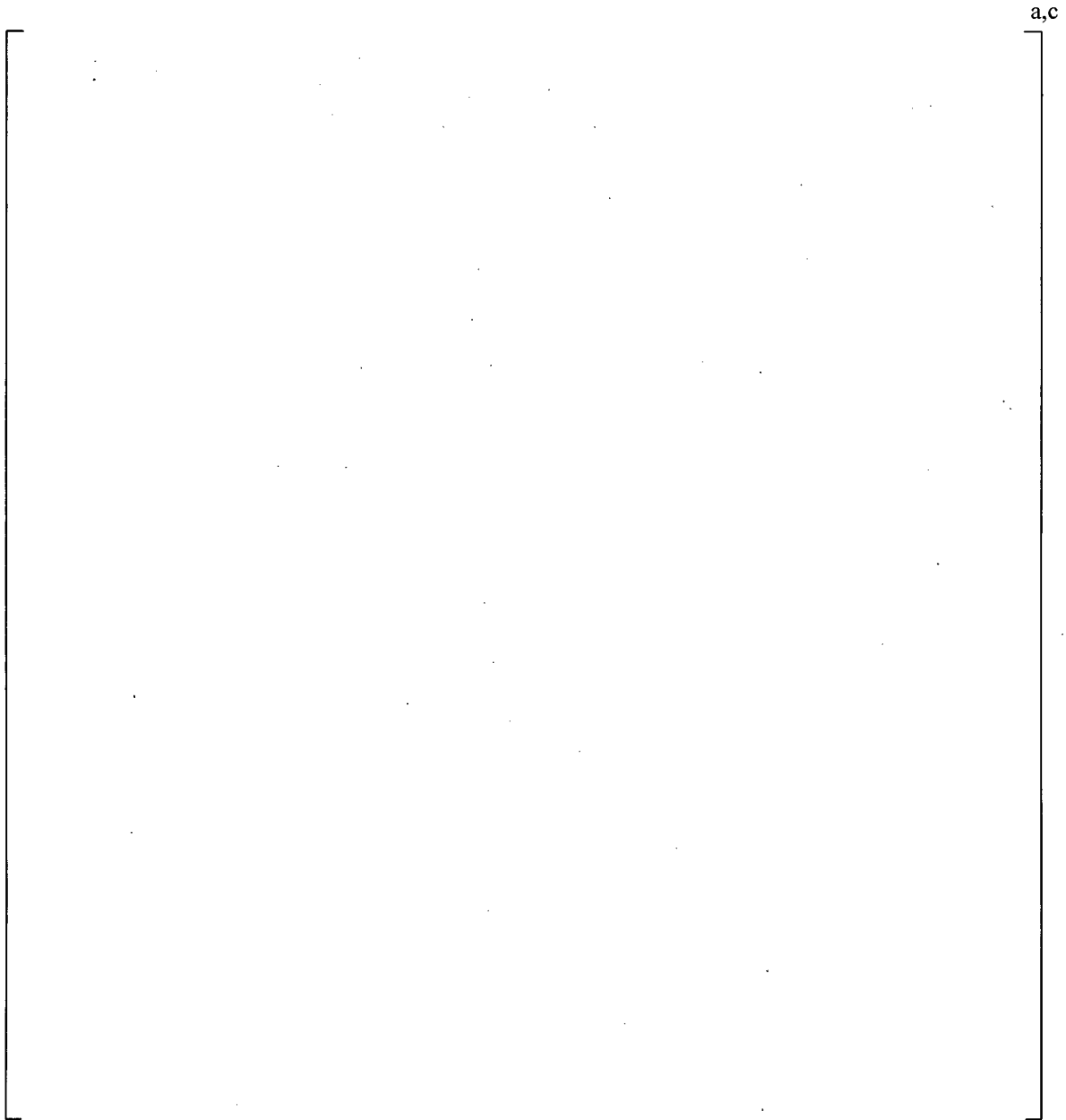


**Figure 3-5 Vane-Bank Geometry**

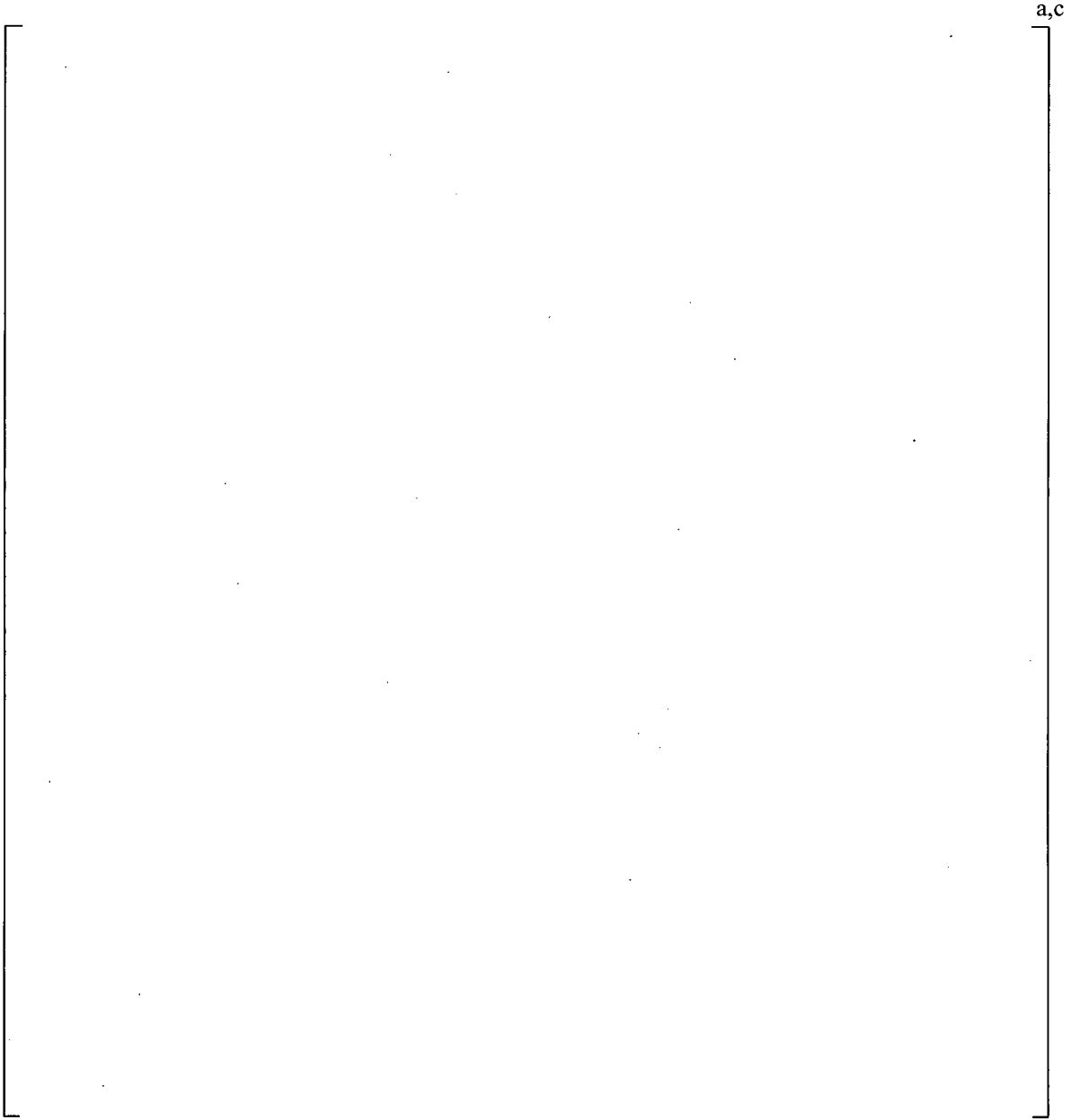


**Figure 3-6 Dryer Hood Geometry**



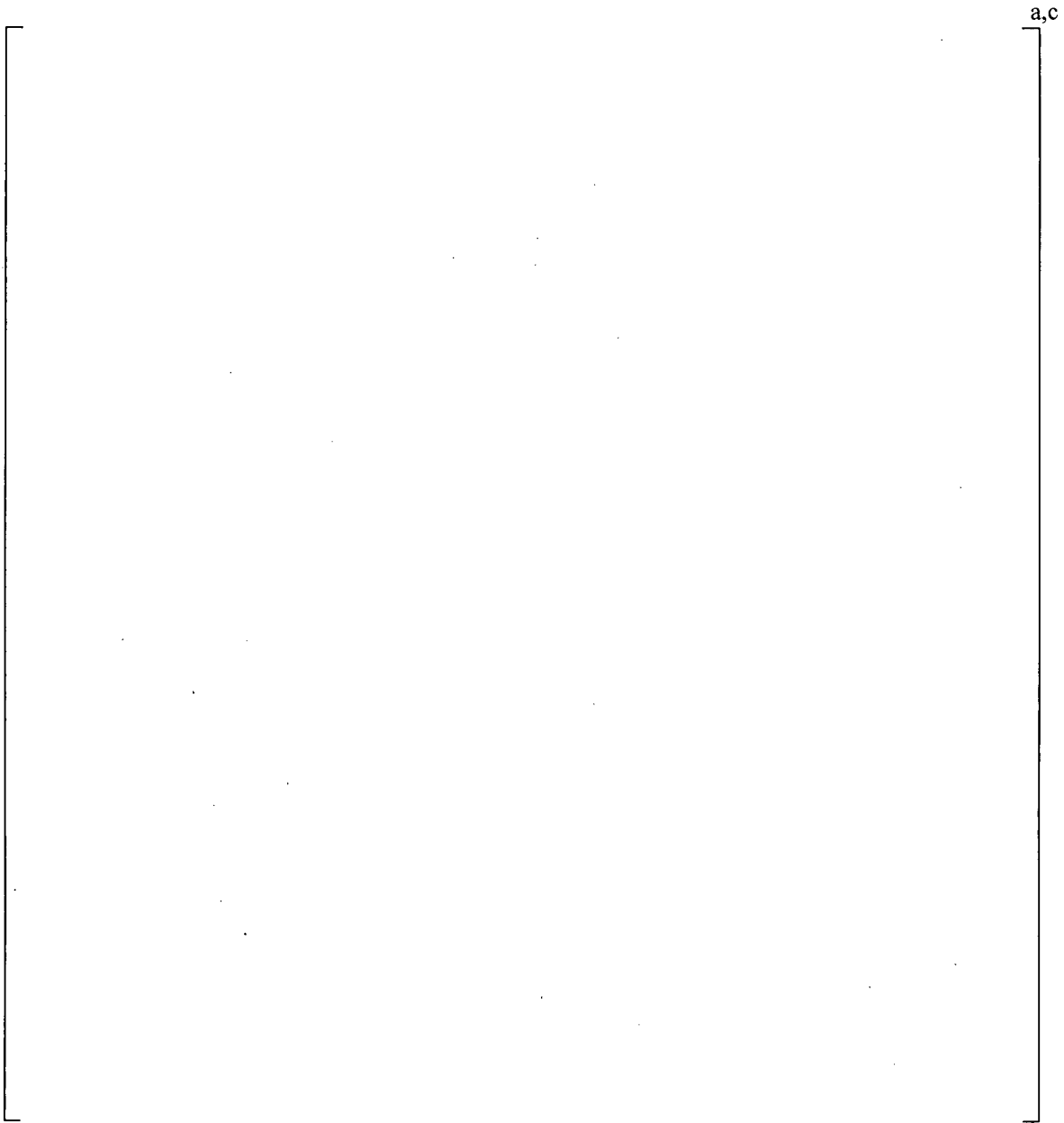


**Figure 3-7 Skirt Geometry**

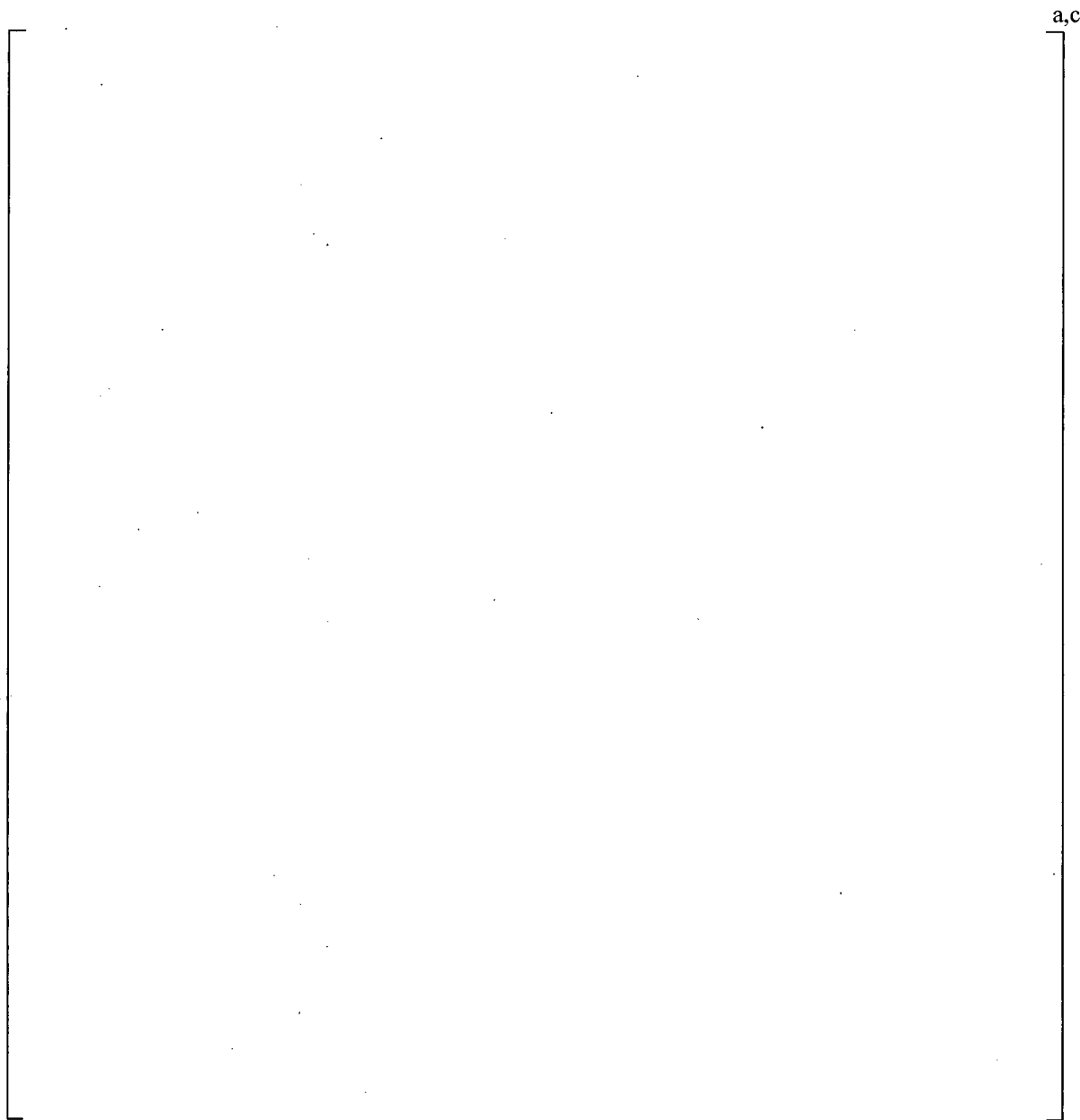


**Figure 3-8 |**

**|<sup>a,c</sup>**

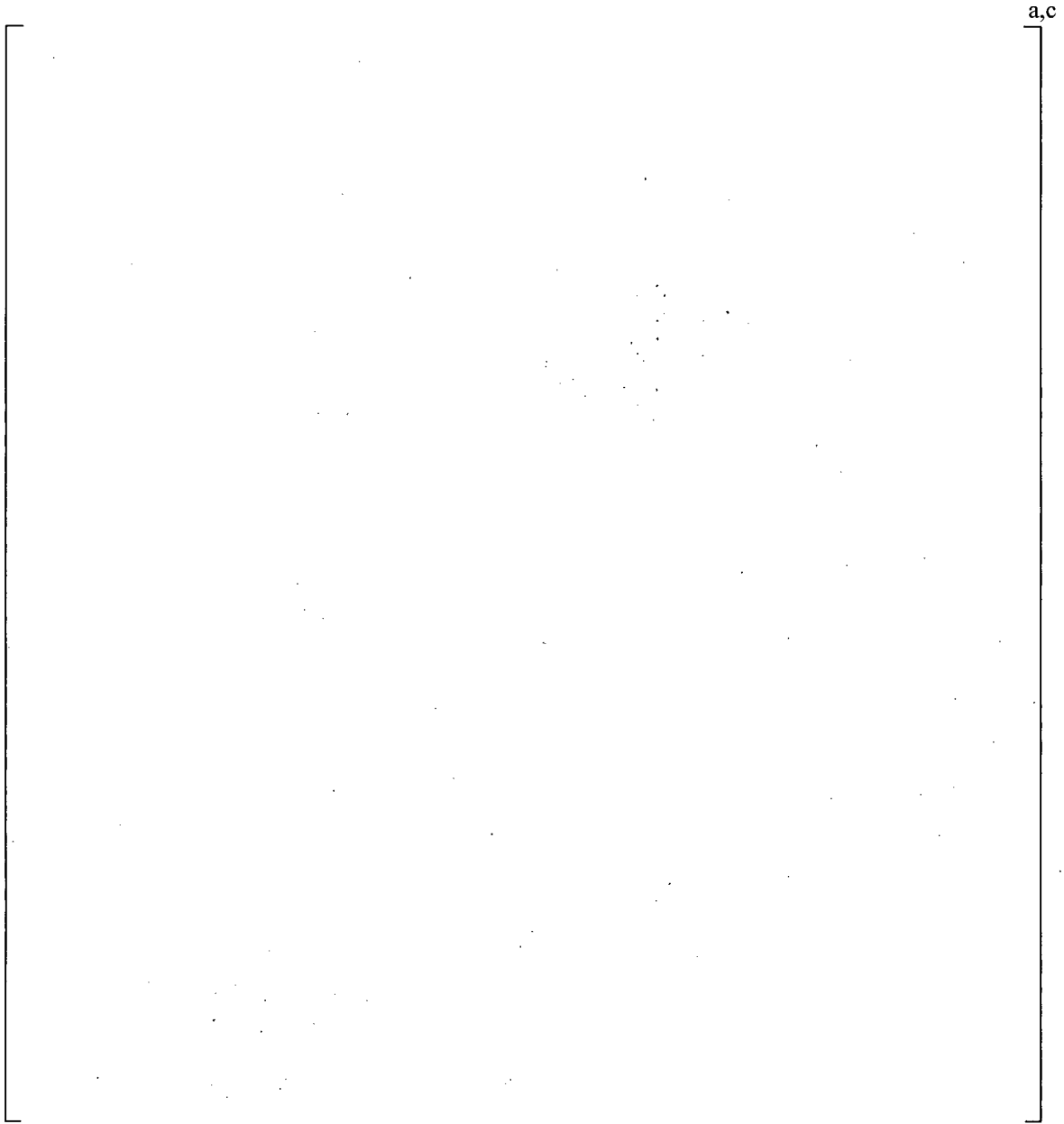


**Figure 3-9 |**

**|<sup>a,c</sup>**

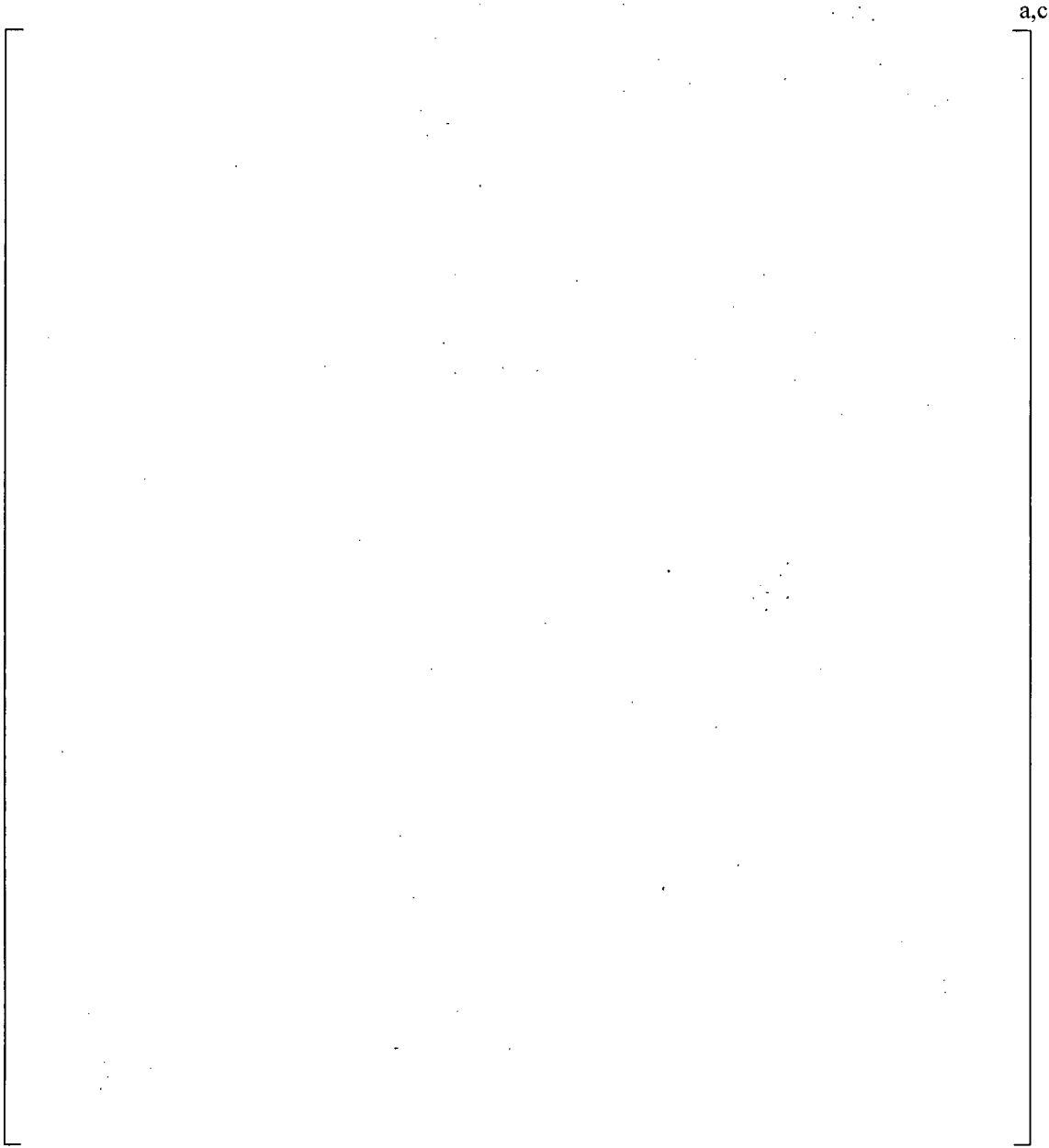


**Figure 3-10** [

] <sup>a,c</sup>

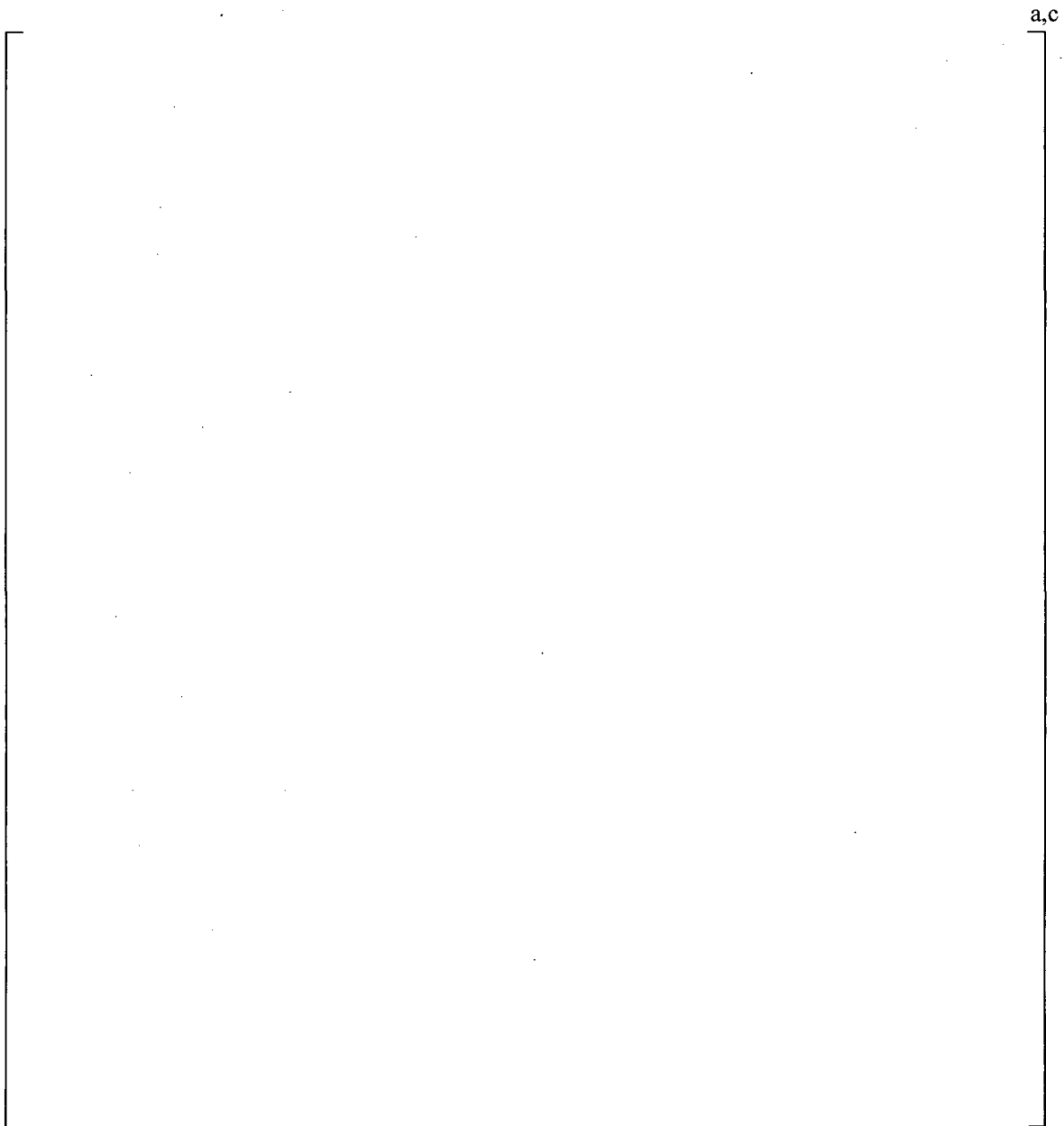


**Figure 3-11 Lifting Lug Geometry**

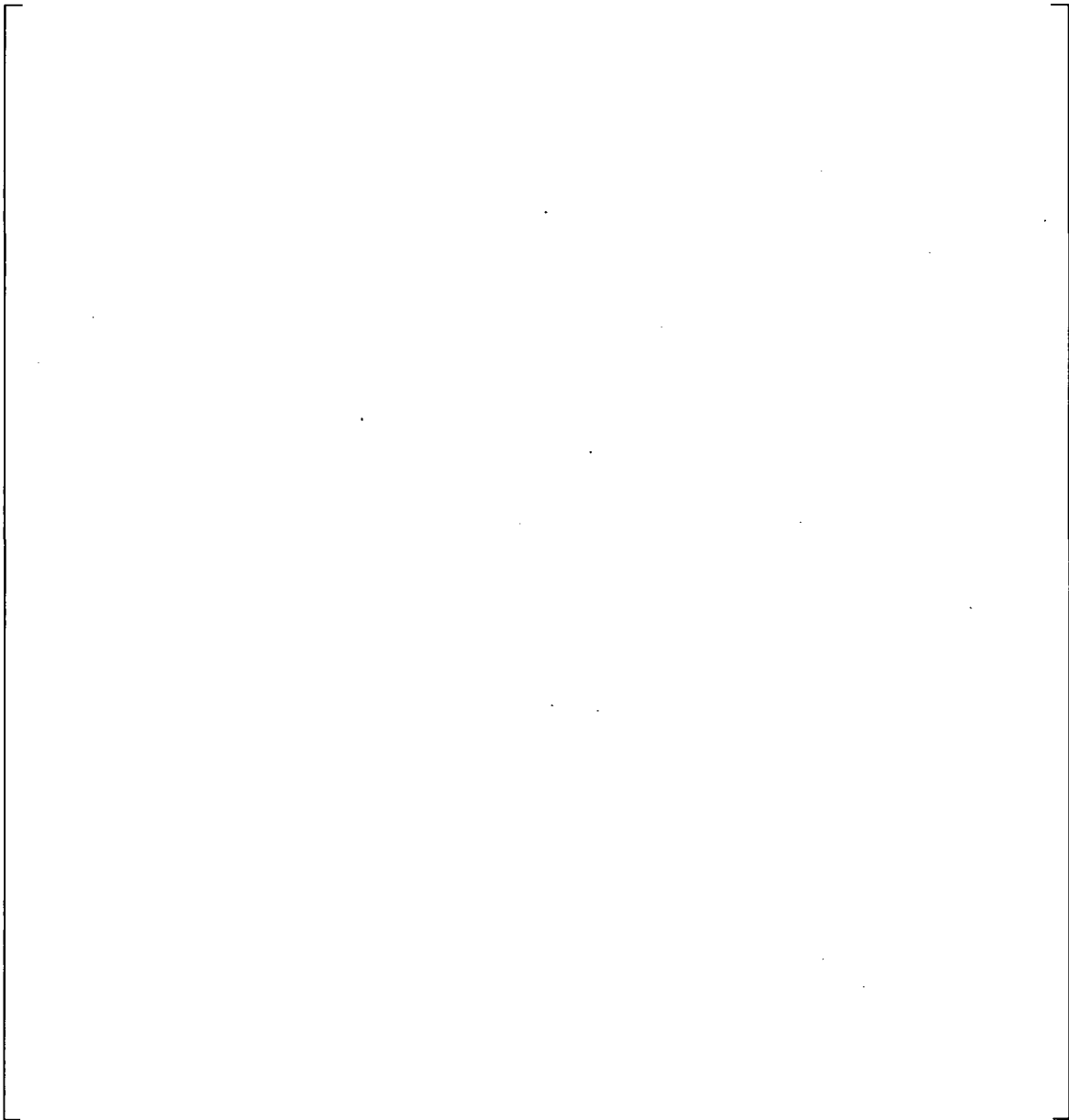
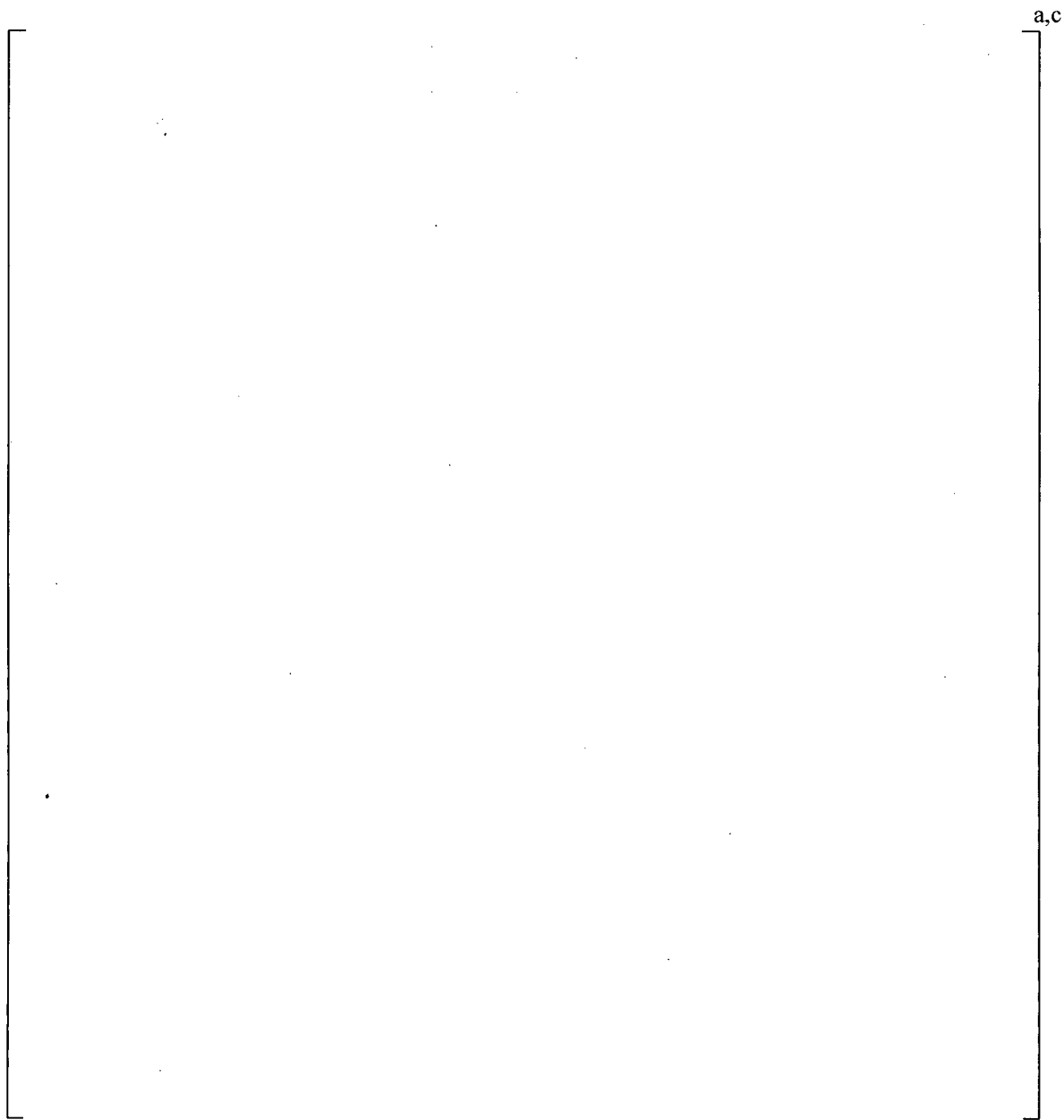


Figure 3-12 [

] <sup>a,c</sup>



**Figure 3-13 |**

**|<sup>a,c</sup>**

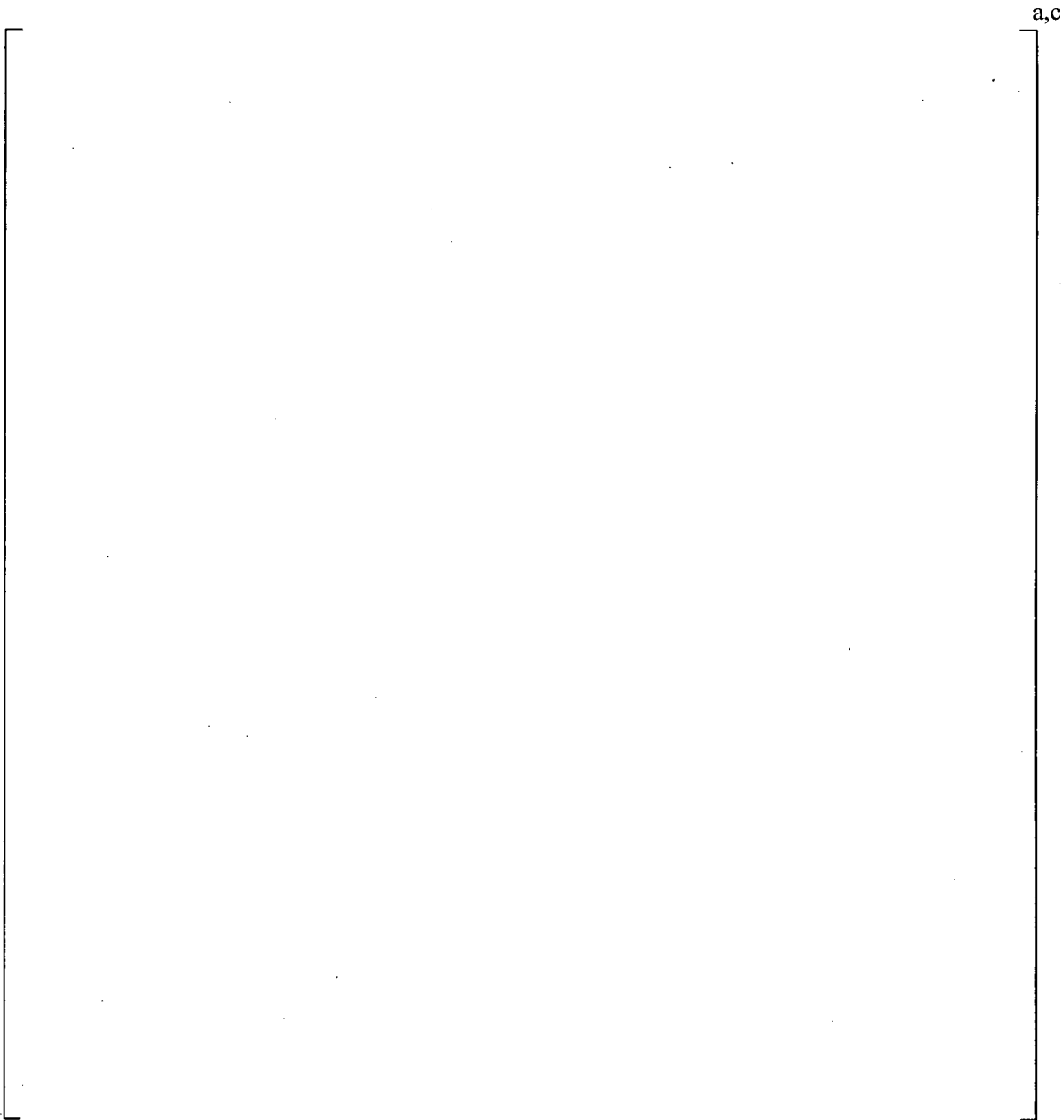


**Figure 3-14** |

|<sup>a, c</sup>



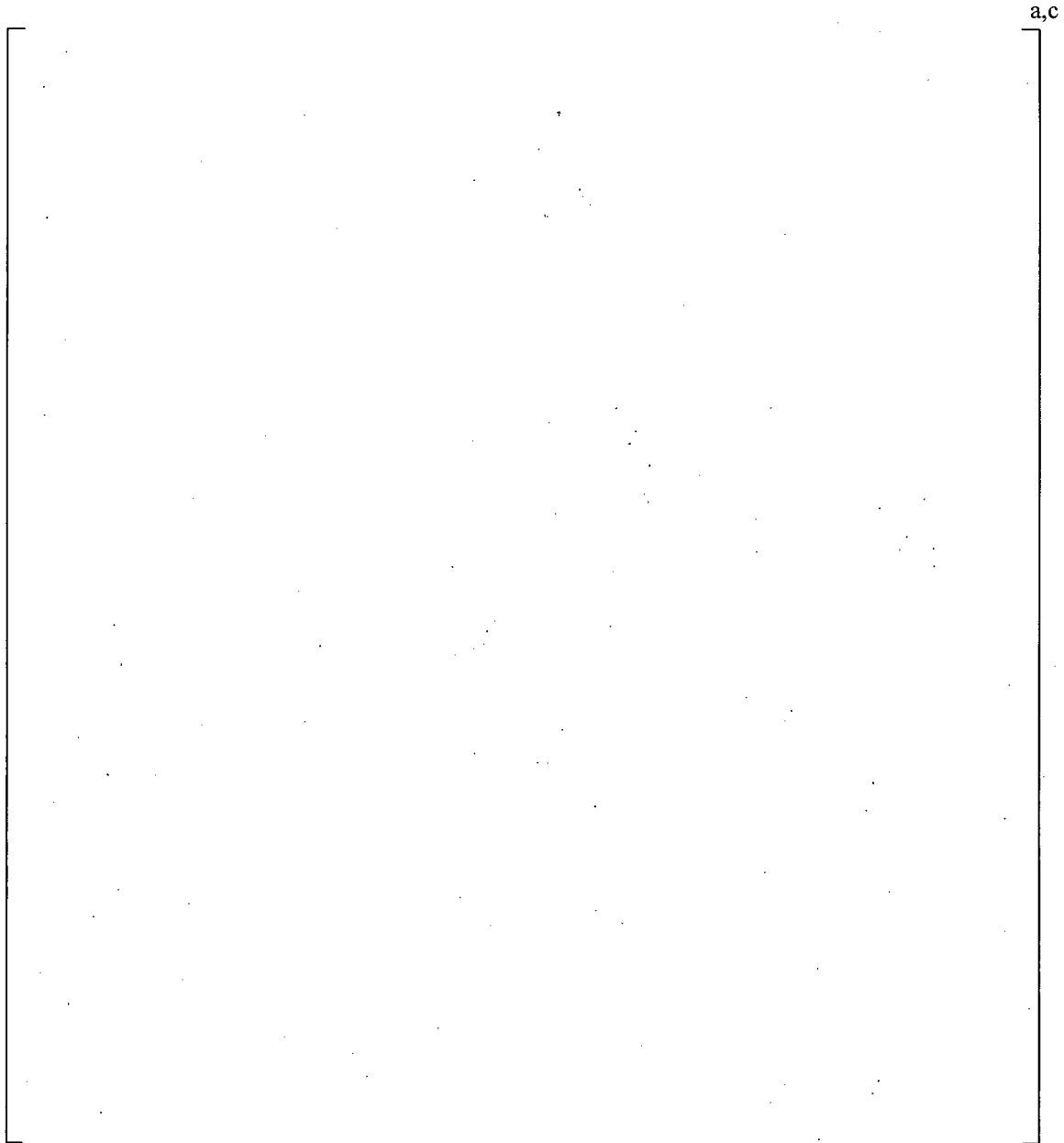


**Figure 3-15** | <sup>a,c</sup>

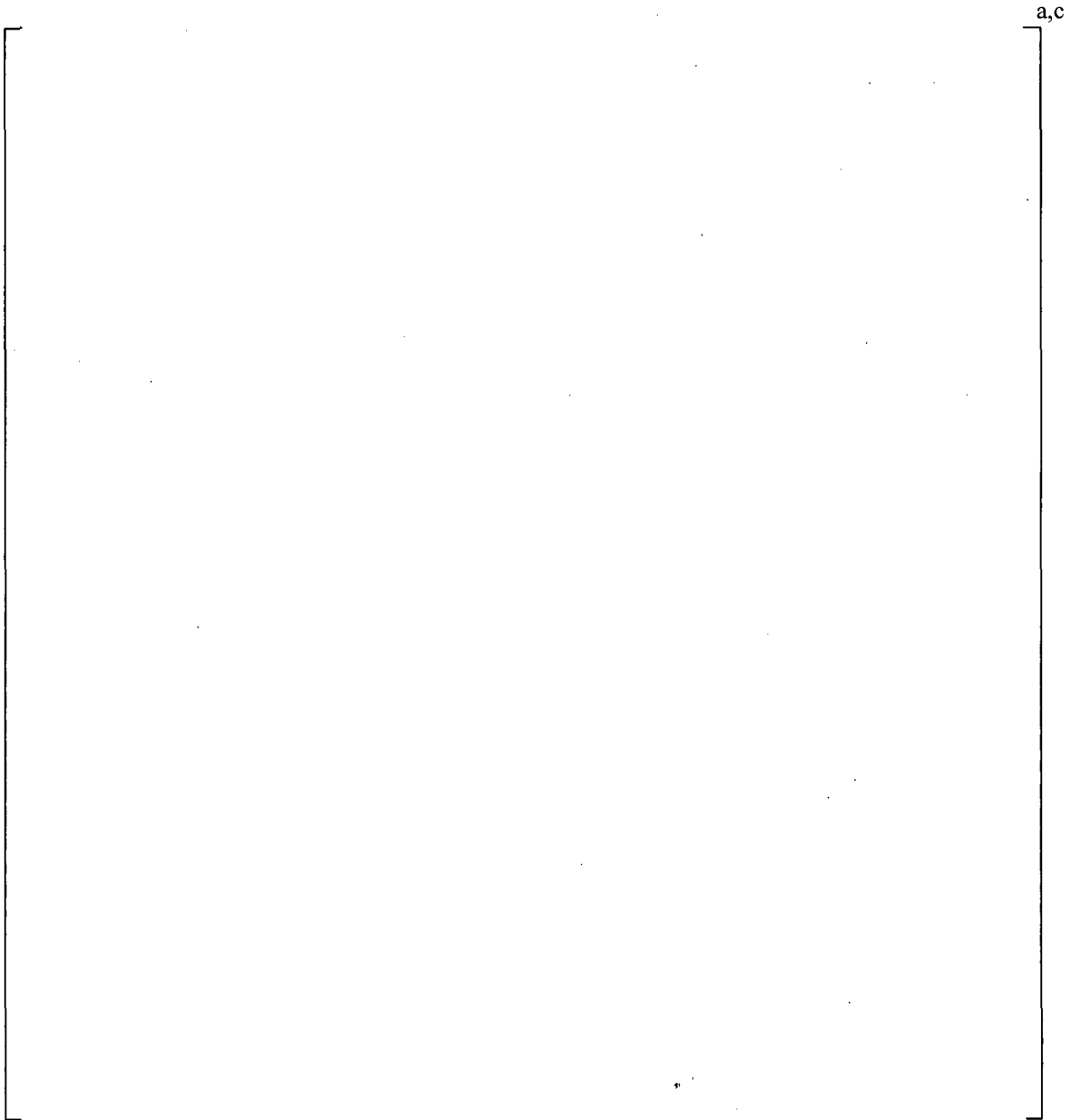


**Figure 3-16 |**

|<sup>a,c</sup>

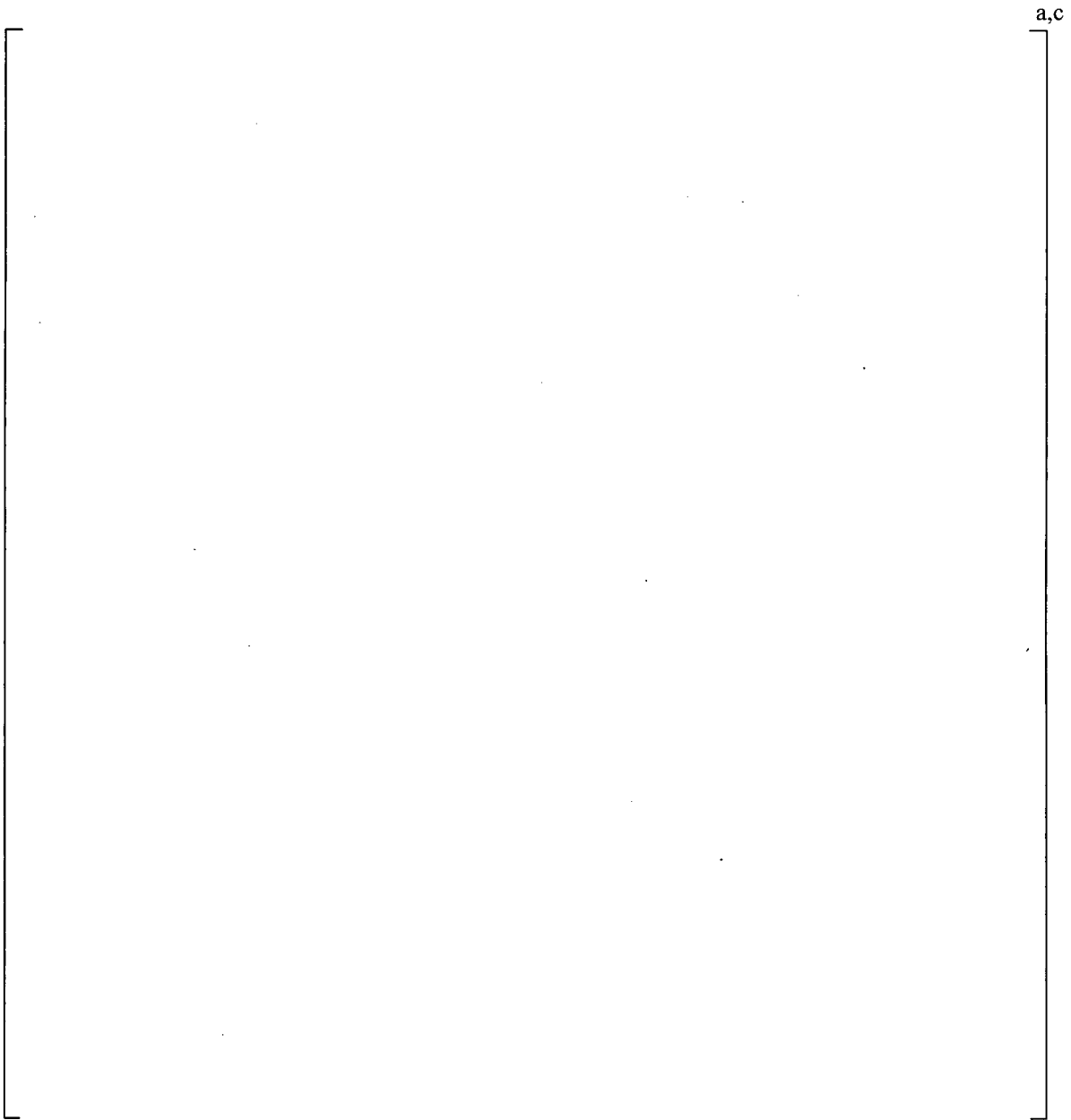


**Figure 3-17 Structural Components of Vane Bank**

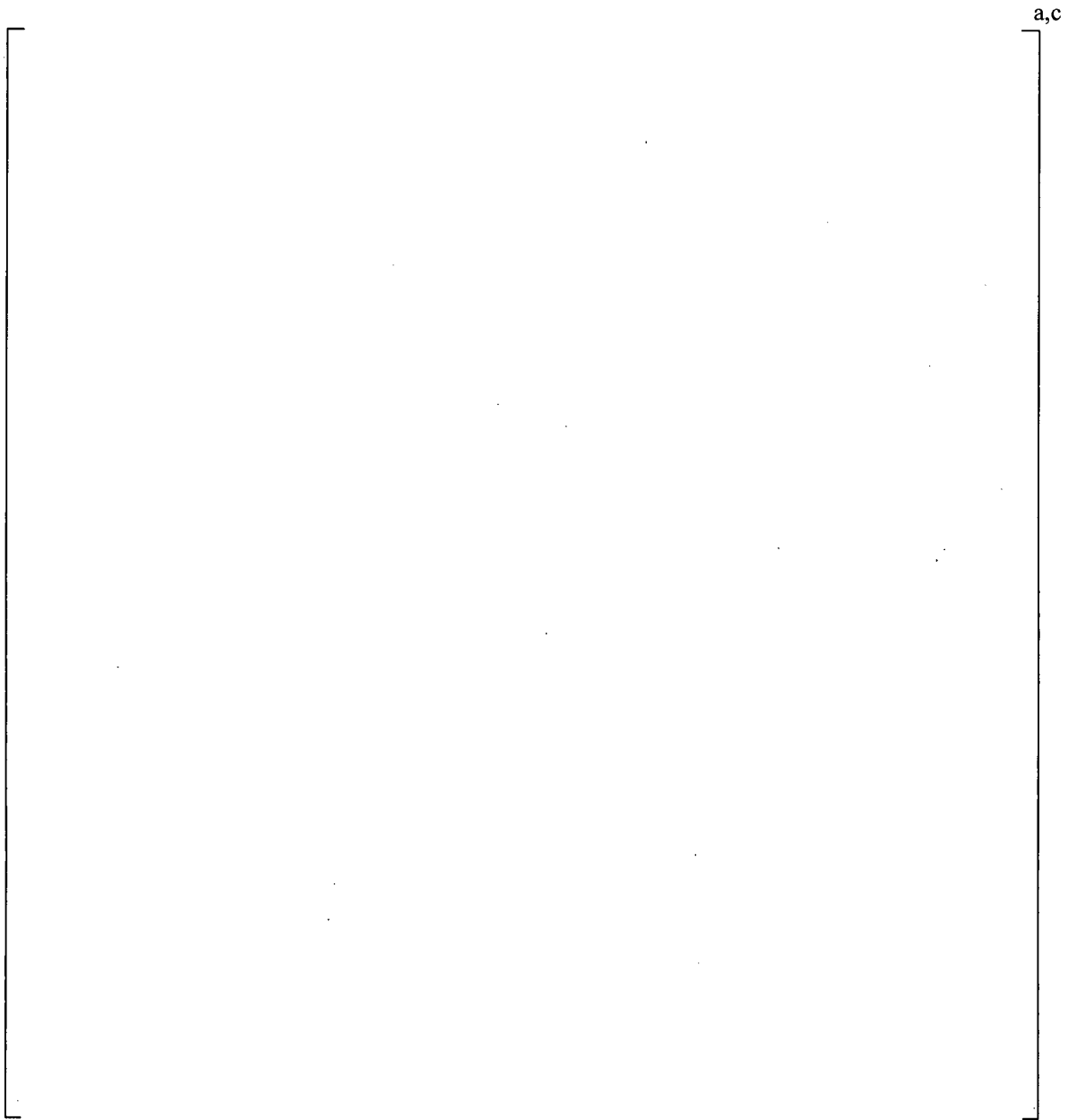


**Figure 3-18 Non-Structural Components of Vane Bank**

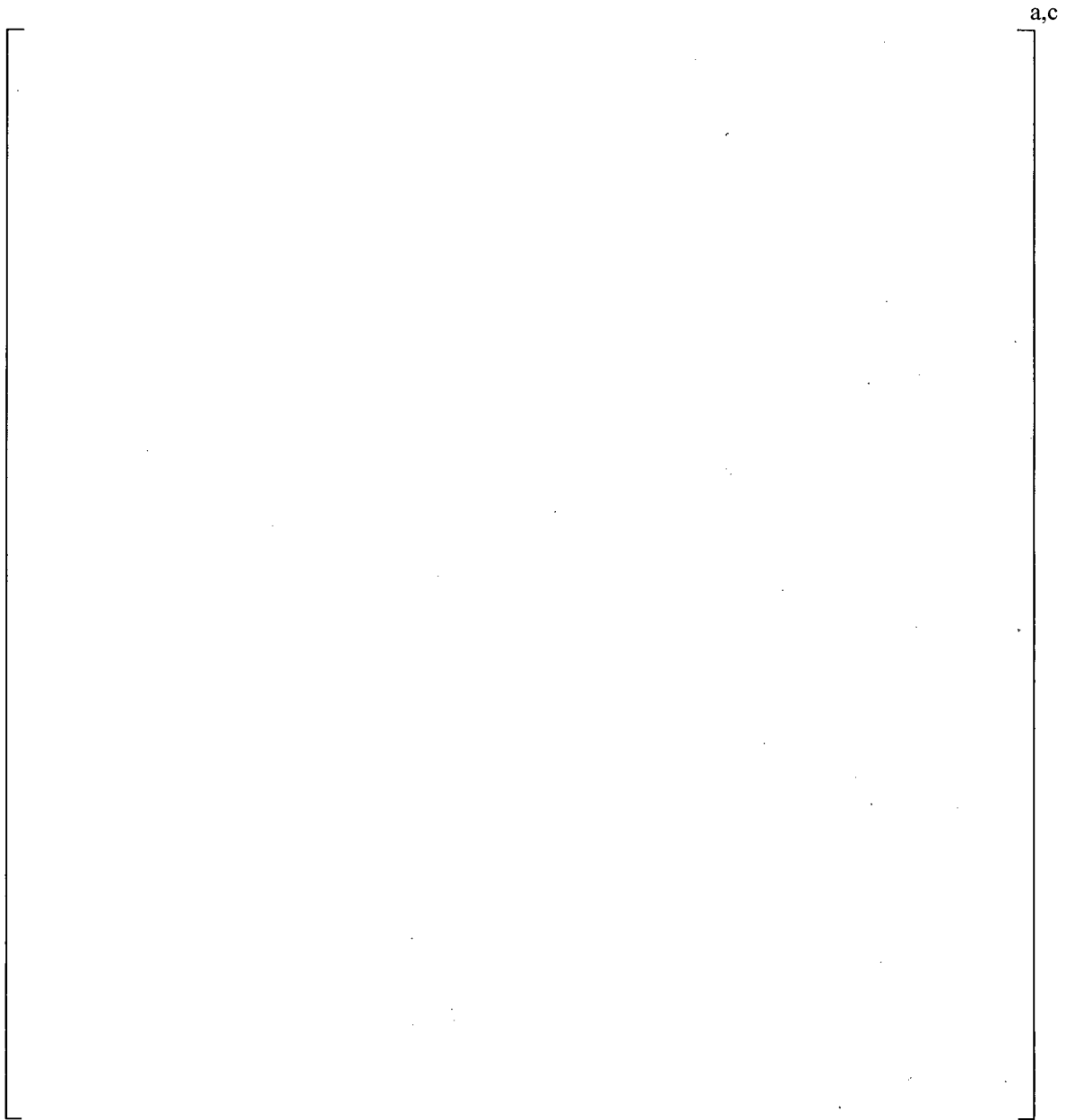


**Figure 3-19 Vane-Bank Mass Blocks**

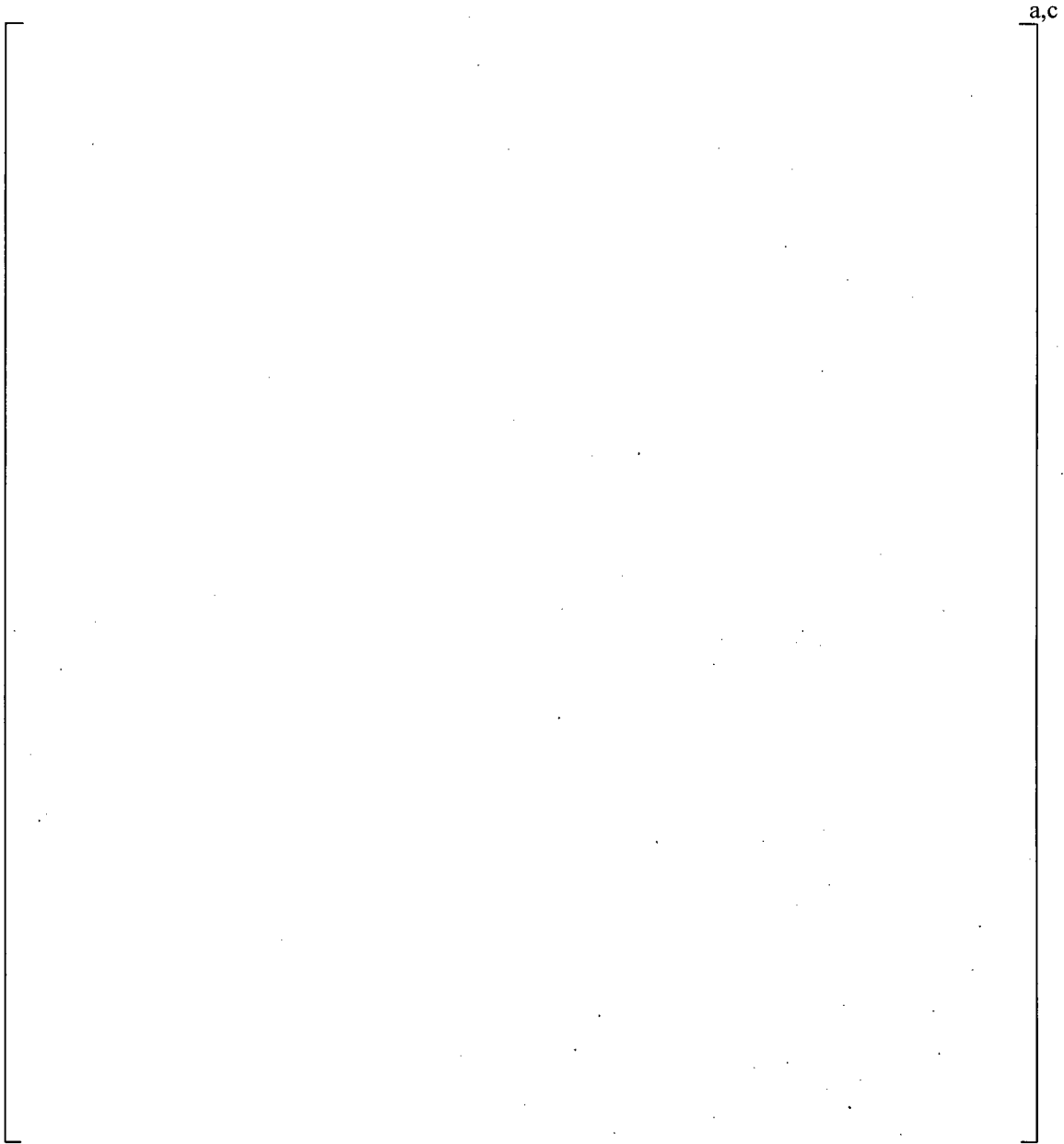


**Figure 3-20 Tie Rod Connection between Mass Blocks and End Plates**

## **4 MATERIAL PROPERTIES**

A summary of the material properties used in the structural analysis is summarized in Table 4-1. Material properties are taken from the ASME Code, Reference 3, for SS316L at a temperature of 575°F. The density of the skirt material below the water is increased to account for hydrodynamic effects of the water. The perforated plates, located at the entrance to the vane banks, are modeled with equivalent plate properties to account for the reduced stiffness and mass of the plates. The density of the solid block representation of the vane banks is adjusted to achieve the correct overall mass of each vane bank.

### **4.1 STRUCTURAL DAMPING**

Structural damping is defined as 1% of critical damping for all frequencies. This damping is consistent with guidance given on page 10 of NRC RG-1.20 (Reference 4). Using the harmonic analysis approach a consistent damping level is used across the frequency domain.

a,c

**Table 4-1      Summary of Material Properties**

--



---

## 5 MODAL ANALYSIS

As a precursor to performing the transient analysis, a modal analysis of the dryer was performed. The modal analysis was performed for modes between 0 Hz and 140 Hz. The fundamental modes for the hood and skirt are shown in Figure 5-1 through Figure 5-8. The fundamental modes for the [ ]<sup>a,c</sup>, respectively.

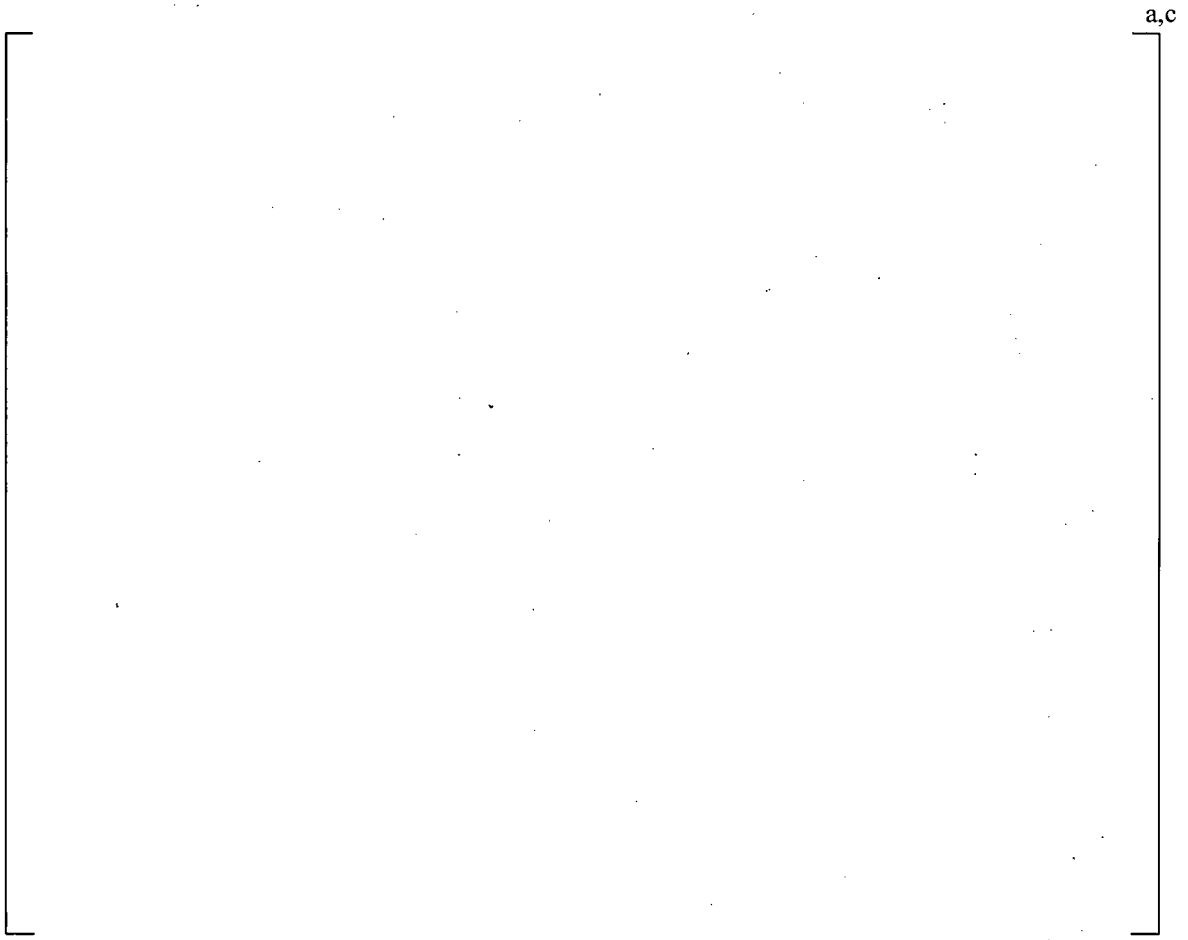


**Figure 5-1 Modal Analysis:** [ ]<sup>a,c</sup>

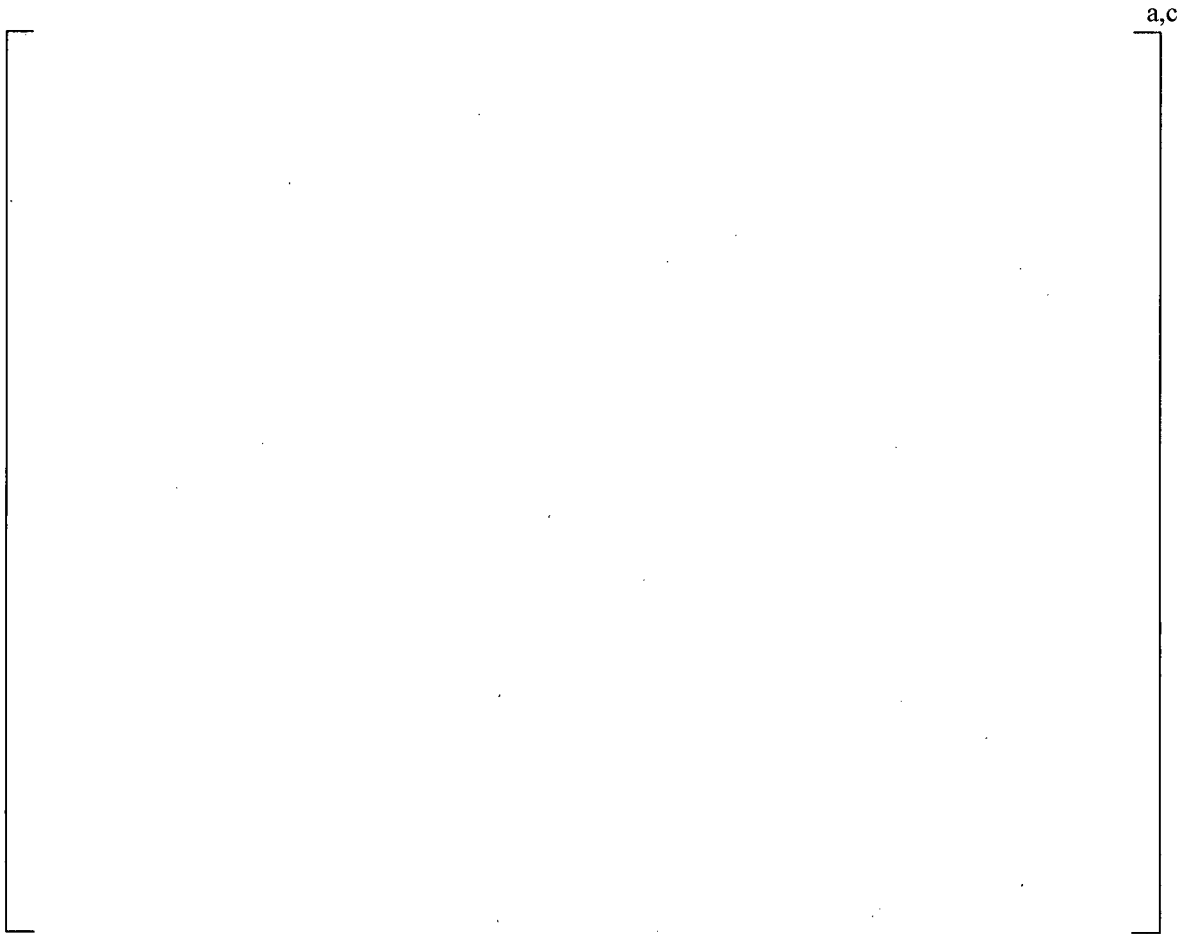
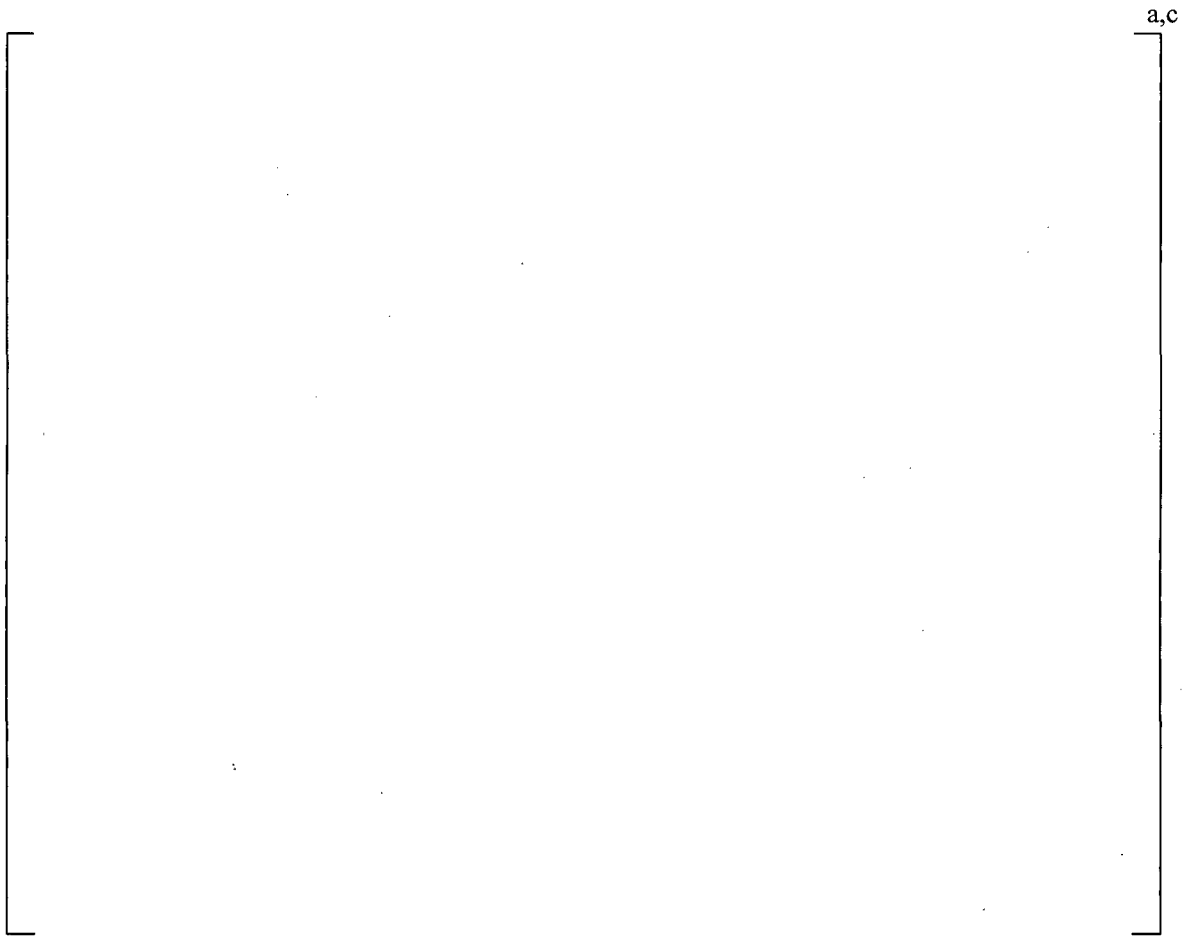


Figure 5-2 Modal Analysis: [ ]<sup>a,c</sup>



**Figure 5-3 Modal Analysis: | ]<sup>a,c</sup>**



**Figure 5-4 Modal Analysis:** |<sup>a,c</sup>



**Figure 5-5 Modal Analysis:** [ ]<sup>a,c</sup>



**Figure 5-6 Modal Analysis:** [ ]<sup>a,c</sup>



**Figure 5-7 Modal Analysis:** | ]<sup>a,c</sup>





Figure 5-8 Modal Analysis: [ ]<sup>a,c</sup>

## 6 LOAD APPLICATION

The frequency-dependent acoustic loads were developed using a three-dimensional (3-D) acoustic model representation of the dryer assembly. The acoustic pressure (P) loads on the steam dryer structure were calculated by solving the 3-D wave diffusion equation in the frequency domain, i.e., the Helmholtz equation.

$$\nabla^2 P(\vec{r}) + k^2 P(\vec{r}) = 0$$

Where  $k = \omega/c$  is the wave number,  $\omega$  is the angular frequency,  $r$  is a spatial variable, and  $c$  is the speed of sound in the medium of interest.

The resulting pressure loads are generated using a 1.5-inch uniform mesh grid. Plots showing the geometry of the acoustic model are provided in Figure 6-1 and Figure 6-2. Loads are developed for both monopole and dipole load sources, and include both the real and imaginary portions of the load in order to maintain phasing information.

The acoustic load files have a frequency increment between solutions of [ ]<sup>ac</sup> Hz. Using special-purpose computer codes, the frequency interval is reduced to limit the peak response error below 5%. This methodology results in variable frequency spacing across the frequency domain, with finer frequency spacing at the lower frequencies.

The acoustic load files generated in the acoustic analysis are input to a special-purpose computer program and the data is reorganized into a 3-D table array format required for reading into ANSYS. The data from the acoustic analysis is limited to the grid positions of the acoustic model and only data adjacent to the steam dryer surfaces is present in the files. In preparing the ANSYS load tables, interpolation of the data on the model surface and simple diffusion schemes off the surface are used to fully populate the load tables.

To be consistent with the acoustic model, only surfaces of the structural FEM that are represented in the acoustic model are prepared to accept the pressure values from the table array files. The FEM is prepared by selecting surfaces common to the acoustic model and superimposing ANSYS pressure (SURF154) elements that are capable of applying both real and imaginary components of the pressure loads.

Even though pressure values fill the entire grid pattern of the table array files, which could translate to every element of the structural FEM having a pressure loading, only the similar structural surfaces represented in the acoustic model receive the pressure loading in the harmonic solution. The data received from the acoustic solution are only at specific surfaces and the spatial interpolation performed is more specific to the immediate area of these surfaces ensuring accurate application of pressures loads.

Figure 6-3 and Figure 6-4 show the orientation of the steam dryer models, both acoustic and structural, relative to plant references for 0-degrees azimuth and MSL locations. Plots showing representative pressure loads for two of the unit load cases are provided in Figure 6-5 and Figure 6-6. Note that these loads are unit load cases, and therefore, the pressure values are relative. The unit loads are subsequently scaled using results from the acoustic circuit model (ACM) discussed below.

To establish scale factors to apply to the unit loads from the Helmholtz acoustic analysis, an analysis is performed that combines [

] <sup>a,c</sup>.

Strain gages were mounted on the four MSLs of Monticello. Two data sets are examined in this analysis. The first data set corresponds to the CLTP power level, and the second set corresponds to the CLTP signals modified with the scaling factors obtained from a one-eighth scale model test performed for Monticello with the replacement dryer to approximate EPU conditions. The resulting scale factors are supplied to the dynamic analysis code in the form of text files: two files for CLTP conditions, corresponding to the monopole and dipole loads; and similarly, two files for EPU conditions.

The scale factors that are obtained from the ACM analysis are related to the frequency sampling rate for the strain gage data collection. In the case of the Monticello plant, the sampling rate was [

] <sup>a,c</sup>.

[

] <sup>a,c</sup>.



**Figure 6-1 Helmholtz Acoustic Model**

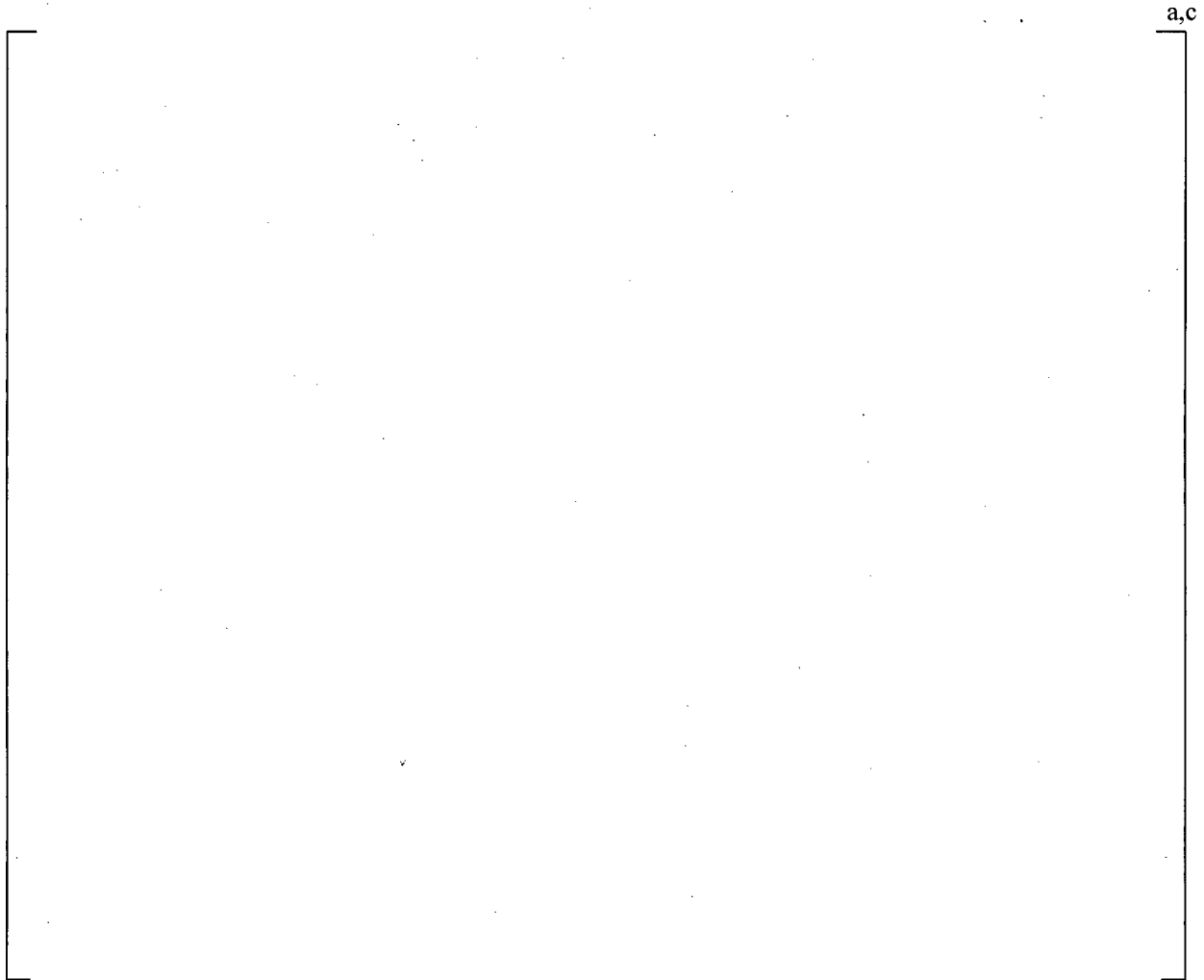
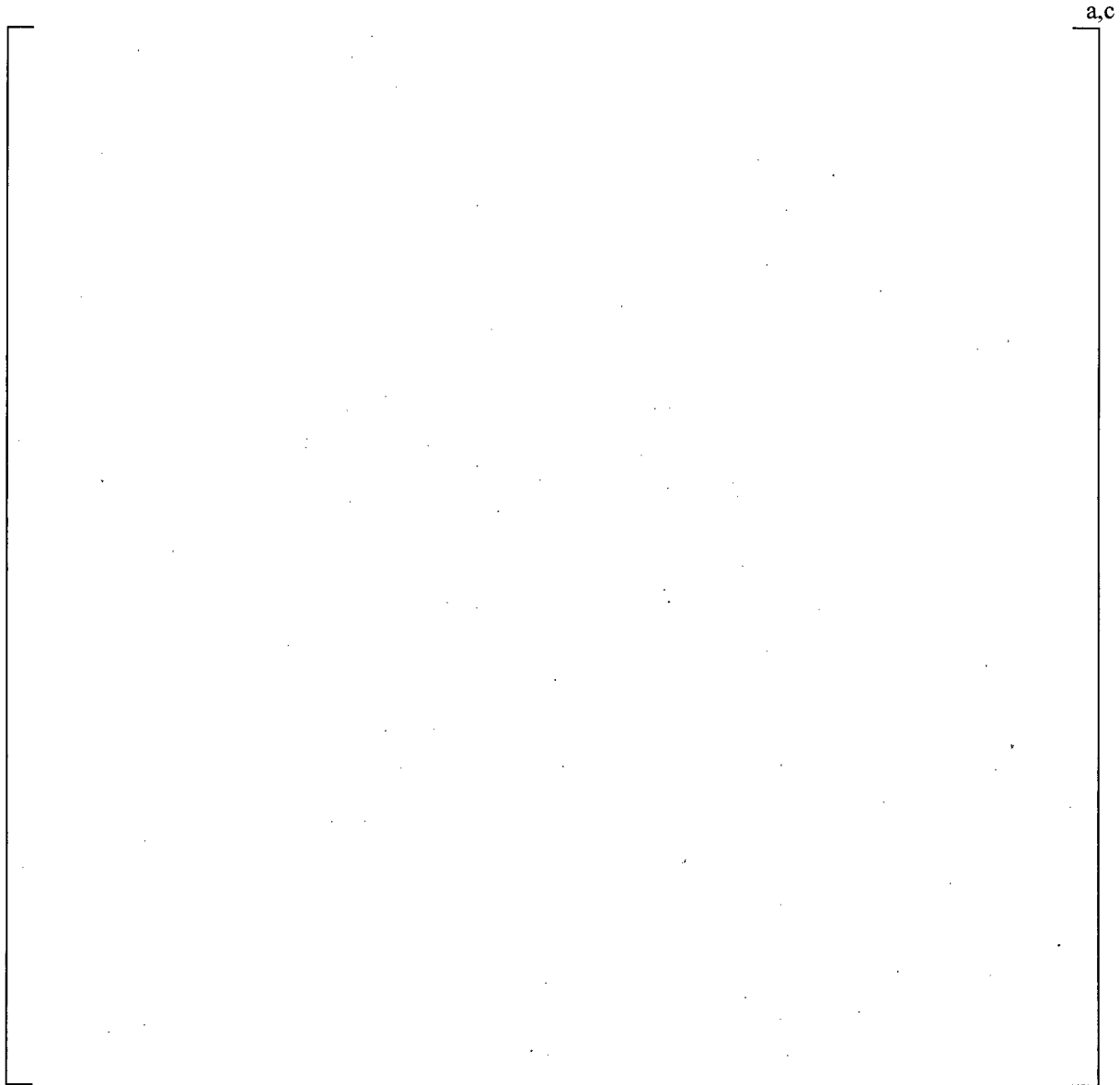
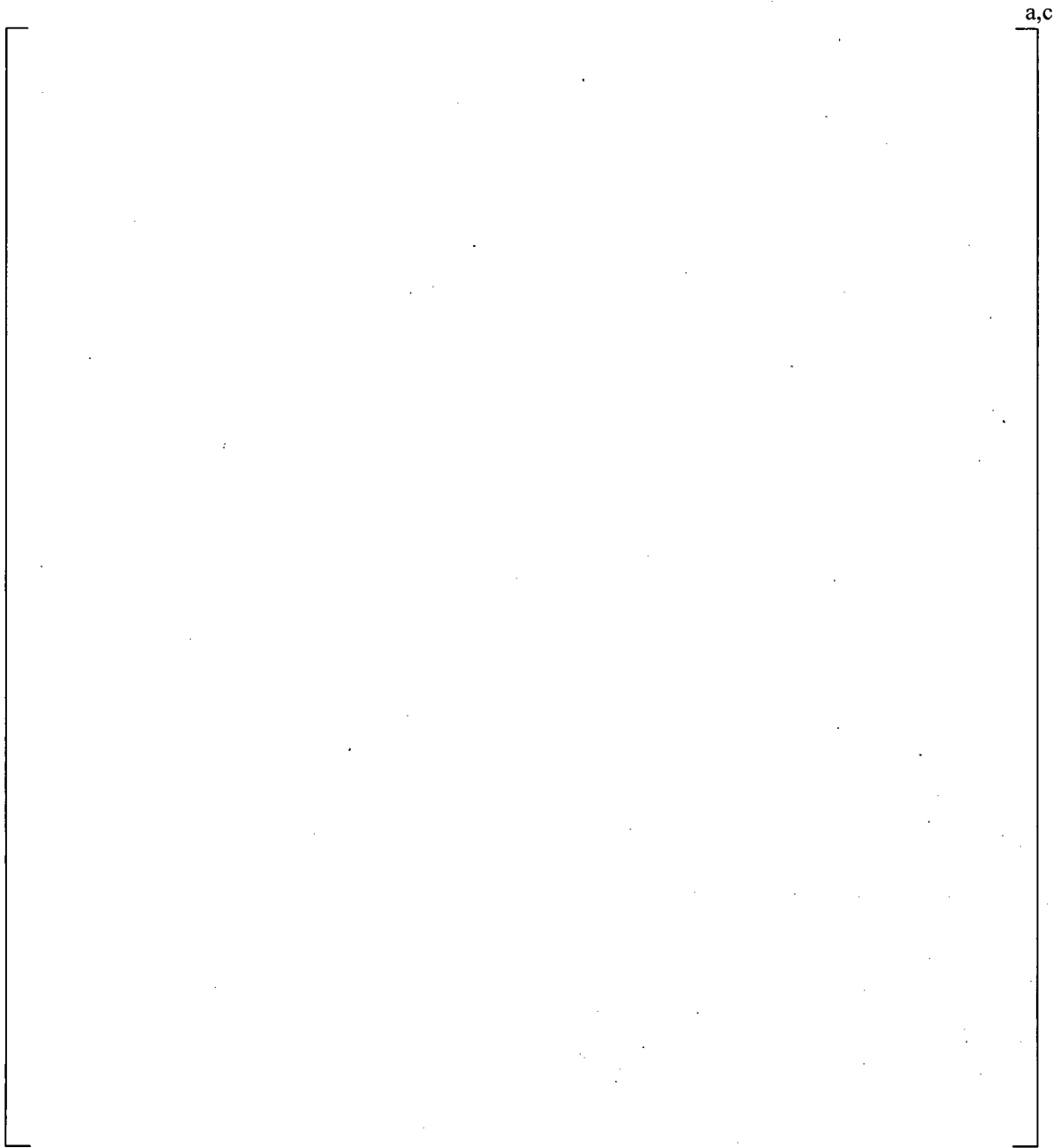


**Figure 6-2 Three-Dimensional Views of the Acoustic Model**



Note: Dimensions are in millimeters. As noted, dimensions in brackets are in inches.

**Figure 6-3 ACM and FEM Global Coordinate System Layout, Top View**



Note: Dimensions are in millimeters. As noted, dimensions in brackets are in inches.

**Figure 6-4 ACM and FEM Global Coordinate System Layout, Section View**



Note: Although the legend shows displacement (UX) as the plotted parameter, the quantities plotted are nodal forces that are calculated internally by ANSYS from the applied pressure loads.

**Figure 6-5 Applied Nodal Forces Due to Unit 60 Hz Load from Main Steam Line-A**





Note: Although the legend shows displacement (UX) as the plotted parameter, the quantities plotted are nodal forces that are calculated internally by ANSYS from the applied pressure loads.

**Figure 6-6 Applied Nodal Forces Due to Unit 94.5 Hz Load from Main Steam Line-D**

---

## 7 STRUCTURAL ANALYSIS

### 7.1 HARMONIC ANALYSIS

#### 7.1.1 Unit Load Harmonic Solutions

Harmonic solutions are obtained using the ANSYS FEM for the following sets of conditions:

- **Model Support (Boundary) Conditions**

The model is supported [

] <sup>a,c</sup>.

- **Operating Conditions**

Two sets of operating conditions, corresponding to CLTP and EPU conditions, are evaluated.

- **Frequency Shifts**

To account for possible uncertainties in the model development relative to predicting component natural frequencies, frequency shifts are applied to the acoustic loads. In addition to the reference conditions, [

] <sup>a,c</sup>.

### 7.1.2 Overview – Time-History Solution

The harmonic analysis begins with the [

] <sup>a,c</sup>. As discussed above, separate solutions are obtained for [

] <sup>a,c</sup>.

[

] <sup>a,c</sup>.

[

] <sup>a,c</sup>.

It was found to be inefficient to process the results [

] <sup>a,c</sup>.

[

] <sup>a,c</sup>.

[

] <sup>a,c</sup>.

---

### 7.1.3 Inverse Fourier Transform

[

]<sup>a,c</sup>.

### 7.1.4 Frequency Scaling (Shifting)

As a result of approximations of the structural interactions used in developing the FEM, small errors can result in the prediction of the component natural frequencies. Varying degrees of mesh discretization can also introduce small errors in the FEM results. To account for these effects, frequency scaling is applied to the applied load history.

If frequency scaling is applied, [

] <sup>a,c</sup>

## 7.2 POST-PROCESSING

### 7.2.1 Primary Stress Evaluation

Once the time-history has been calculated [ ] <sup>a,c</sup>, an evaluation is performed to calculate the maximum alternating stress intensity. The stress intensities for the [

] <sup>a,c</sup>.

For a two-dimensional stress field, the principal stresses are calculated as follows (the X-Y plane is used as an example. The same algorithms are also applicable to other planes.)

$$\sigma_{1,2} = \frac{\sigma_x + \sigma_y}{2} \pm \sqrt{\left(\frac{\sigma_x - \sigma_y}{2}\right)^2 + (\sigma_{xy})^2}$$

$$\sigma_3 = 0.0$$

$$\text{Stress Intensity} = \text{Maximum} \begin{matrix} |\sigma_1 - \sigma_2| \\ |\sigma_2 - \sigma_3| \\ |\sigma_3 - \sigma_1| \end{matrix}$$

For a general 3-D state of stress, the resulting principal stresses correspond to the roots of the following cubic equation as:

$$\sigma^3 - a_2\sigma^2 + a_1\sigma - a_0 = 0$$

where,

$$a_2 = \sigma_x + \sigma_y + \sigma_z$$

$$a_1 = \sigma_x\sigma_y + \sigma_y\sigma_z + \sigma_z\sigma_x - \sigma_{xy}^2 - \sigma_{yz}^2 - \sigma_{zx}^2$$

$$a_0 = \sigma_x\sigma_y\sigma_z + 2\sigma_{xy}\sigma_{yz}\sigma_{zx} - \sigma_x\sigma_{yz}^2 - \sigma_y\sigma_{zx}^2 - \sigma_z\sigma_{xy}^2$$

### 7.2.2 Alternating Stress

The calculation of the alternating stress intensity, following the ASME Code process, is performed as follows:

1. Apply the stress concentration factors (geometric or FSRF), as applicable, to the component stresses.
2. Calculate the range of stress for each component of stress for two time points.
3. Calculate the stress intensity of the component ranges.

[

] <sup>a,c</sup>.

### 7.3 CALCULATION AND EVALUATION OF WELD STRESSES

Due to the nature of the dynamic analysis, detailed modeling of the welds is not practical in the global dryer FEM. Calculation of weld stresses requires a different approach. For the Monticello replacement steam dryer, [

] <sup>a,c</sup>.

As discussed above, detailed weld stresses are not directly available from the finite element analysis.

[

] <sup>a,c</sup>.

[

] <sup>a,c</sup>.

#### **7.4 SUBMODELING TECHNIQUES**

Due to the nature of the acoustic analysis and the large number of unit solutions that are required, it is not practical to use a fine mesh for the acoustic analysis. Rather a mesh density that can accurately predict the dynamic characteristics of the structure is used, but may require some additional analysis for localized

regions of high stress. For areas where additional analysis is necessary using a more refined element mesh, a technique known as submodeling is used. The submodeling method [

7.5 [ ]  
[ ]

]a,c

]a,c

]a,c





**Figure 7-1** [ ]<sup>a,c</sup>

## 8 ANALYSIS RESULTS

### 8.1 GLOBAL MODEL

As discussed previously, the global model was analyzed for both CLTP and EPU conditions, [

In reviewing the analysis results, the primary focus was to establish the limiting conditions for EPU conditions, and then to review the CLTP stresses for a comparison of the effect of increasing to EPU.

[

] <sup>a,c</sup>.

A summary [

] <sup>a,c</sup>.

To show the general distribution of stress, stress contour plots for a number of the components are provided in Figure 8-4 through Figure 8-12.

### 8.2 SUBMODELING

Based on the results for the global model, [

] <sup>a,c</sup>. These are [ ] <sup>a,c</sup> areas where high stresses were observed in the global model.<sup>3</sup>

#### 8.2.1 [ ] <sup>a,c</sup>

[

---

<sup>2</sup> [

<sup>3</sup> [

] <sup>a,c</sup>

] <sup>a,c</sup>

]a,c.

8.2.2 [ ]a,c

[

]a,c.

8.3 [ ]a,c

[

]a,c.

a,c

Table 8-1	Maximum of	<sup>a,c</sup> for EPU Conditions

– Continued –

Table 8-1 (cont.)	Maximum of [	] <sup>a,c</sup> for EPU Conditions

a,c

Table 8-2	Maximum of [	] <sup>a,c</sup> for CLTP Conditions
-----------	--------------	--------------------------------------

– Continued –

Table 8-2 (cont.)	Maximum of	<sup>a,c</sup> for CLTP Conditions

a,c

Table 8-3	Summary of Results –	<sup>a,c</sup> – CLTP Conditions



Table 8-4	Summary of Results – [	] <sup>a,c</sup> – EPU Conditions

a,c

Table 8-5	Summary of Results – I	I <sup>a,c</sup> – CLTP Conditions

a,c

Table 8-6	Summary of Results –	<sup>a,c</sup> – EPU Conditions

a,c

Table 8-7	Summary of Results –	<sup>a,c</sup> – CLTP Conditions

Table 8-8	Summary of Results – [	] – EPU Conditions



**Figure 8-1 Effect of Frequency Shift on Stress Intensity: [ EPU Operating Conditions**

] a.c.



**Figure 8-2 Effect of Frequency Shift on Stress Intensity: [ EPU Operating Conditions**

]<sup>a,c</sup>



**Figure 8-3 Stress Intensity Comparison between EPU and CLTP Conditions**





**Figure 8-4 EPU Stress Intensity Results:** [ ]<sup>a,c</sup>



Figure 8-5 EPU Stress Intensity Results: |<sup>a,c</sup>



**Figure 8-6 EPU Stress Intensity Results: |**

**|<sup>a,c</sup>**



**Figure 8-7 EPU Stress Intensity Results: |** <sup>a.c</sup>

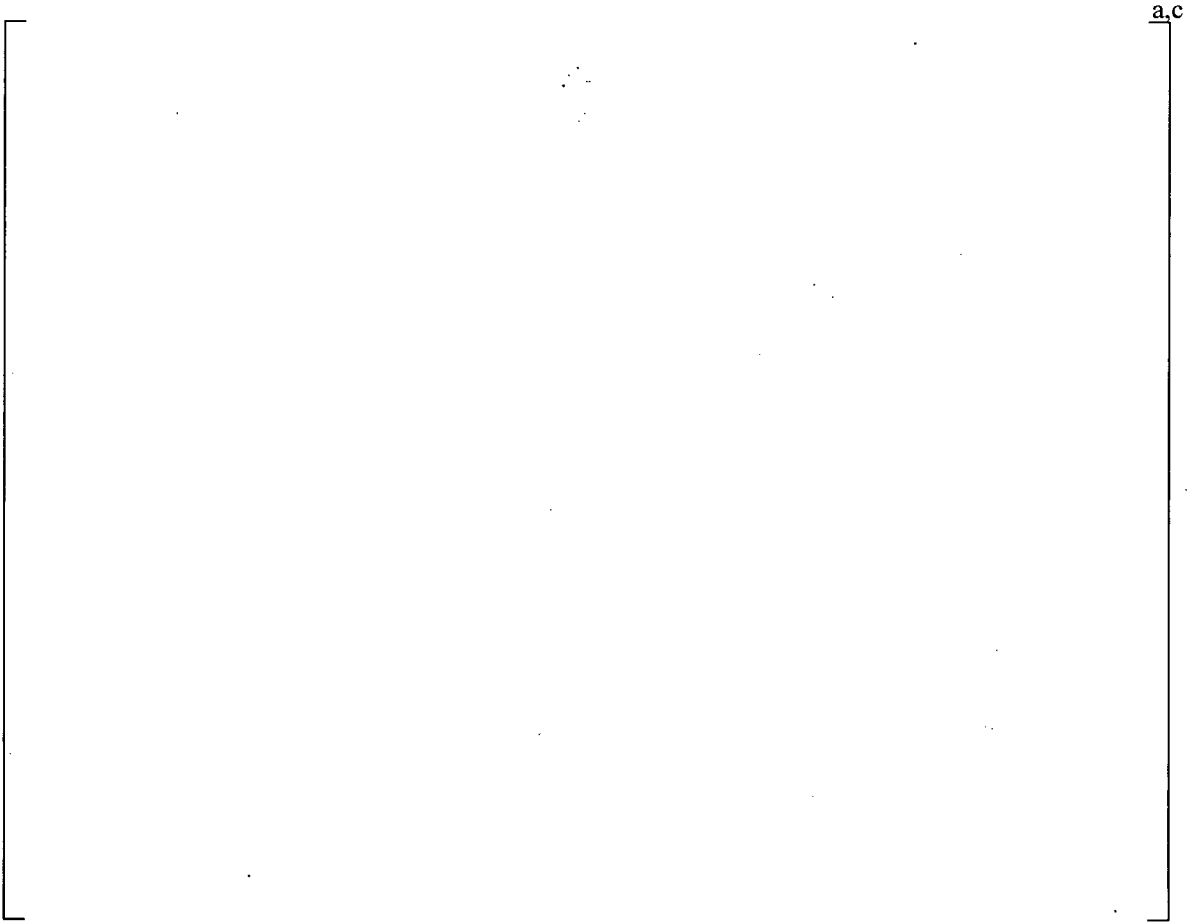


**Figure 8-8 EPU Stress Intensity Results: [ ]<sup>a,c</sup>**



**Figure 8-9 EPU Stress Intensity Results:** [ ]<sup>a,c</sup>

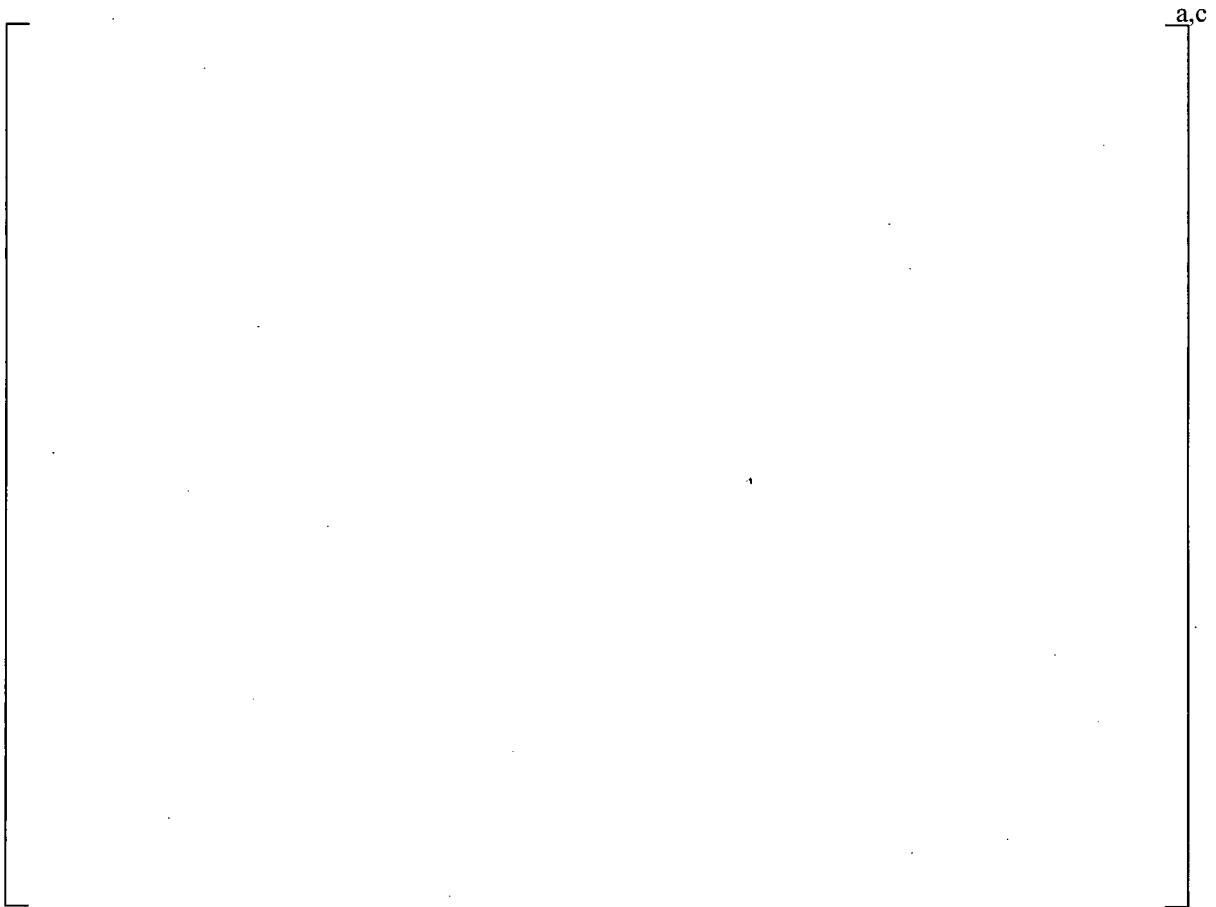


**Figure 8-10 EPU Stress Intensity Results: |**

**|<sup>a,c</sup>**



**Figure 8-11 EPU Stress Intensity Results: |**

|<sup>a,c</sup>





**Figure 8-12 Stress Intensity Results:** |<sup>a,c</sup>



a,c

**Figure 8-13 |**

| a,c



Note: Submodel is shown in yellow.

**Figure 8-14** [

] a,c



Note: Submodel is shown in yellow.

Figure 8-15 |

|<sup>a,c</sup>

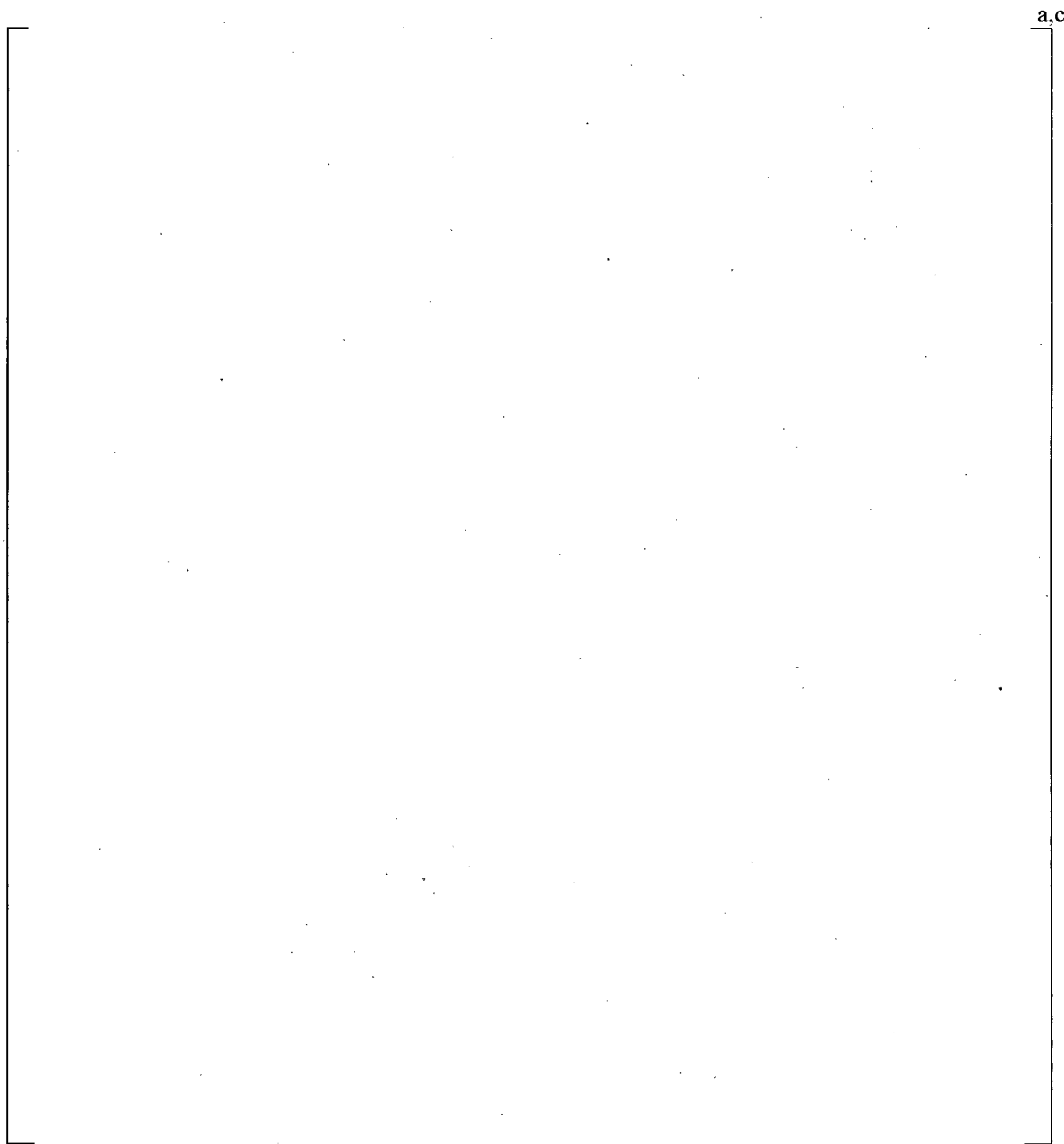


**Figure 8-16** [

] <sup>a,c</sup>



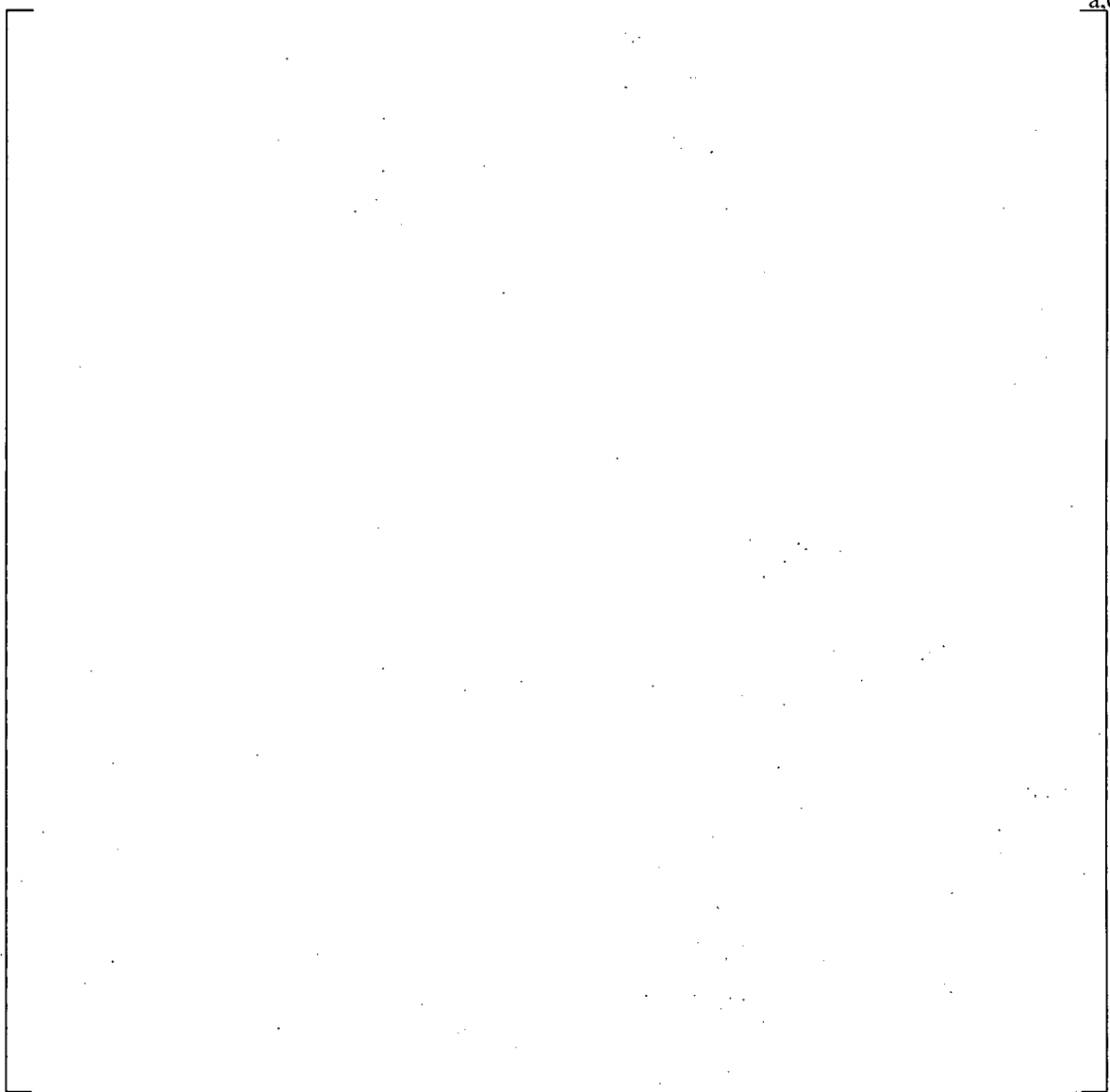
**Figure 8-17 |**

]<sup>a,c</sup>



**Figure 8-18 |**

|<sup>a,c</sup>



a,c

**Figure 8-19** |

|<sup>a,c</sup>



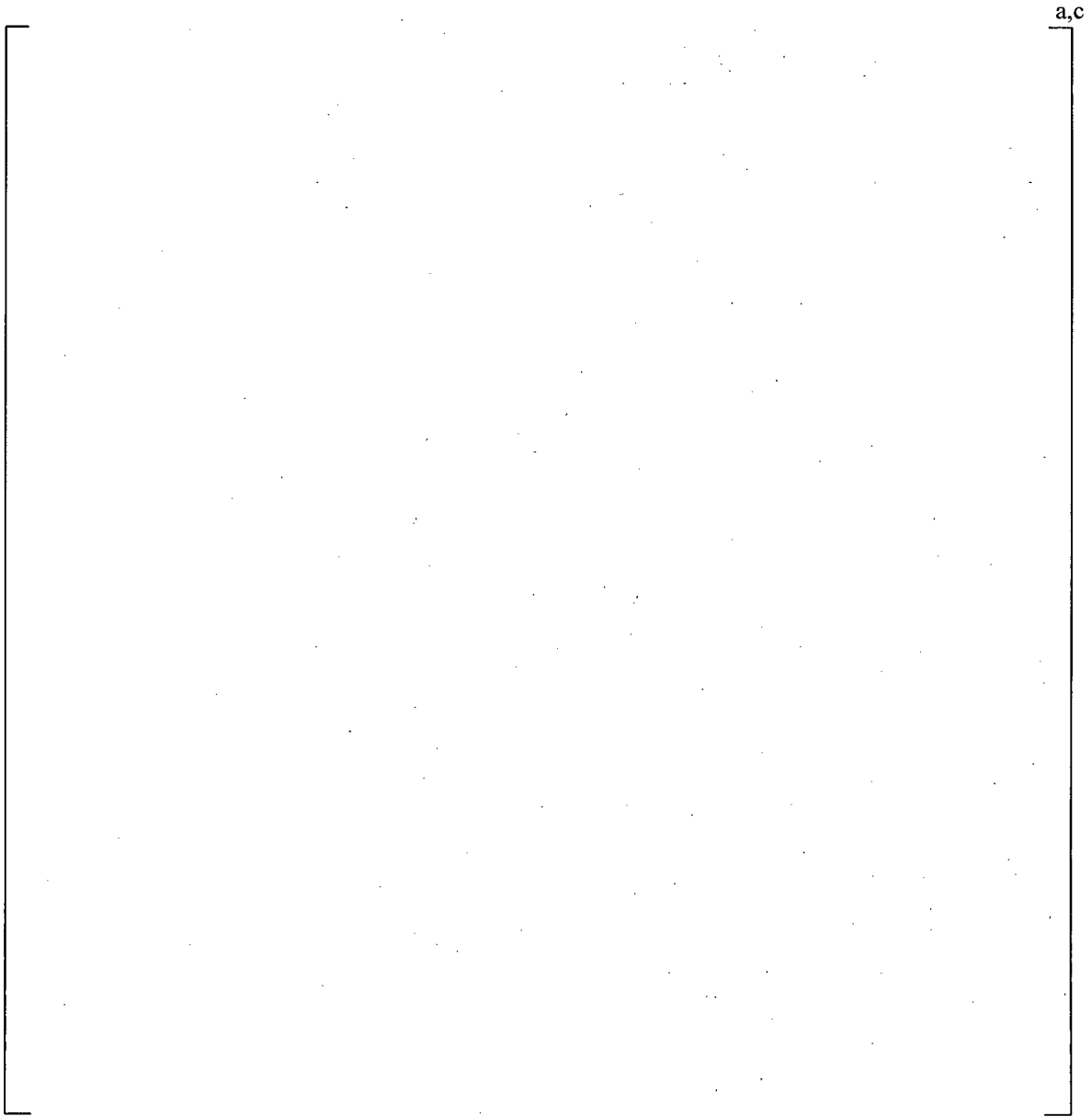


**Figure 8-20** |

|<sup>a,c</sup>



Figure 8-21 [

] <sup>a,c</sup>



**Figure 8-22 [**

**] <sup>a,c</sup>**

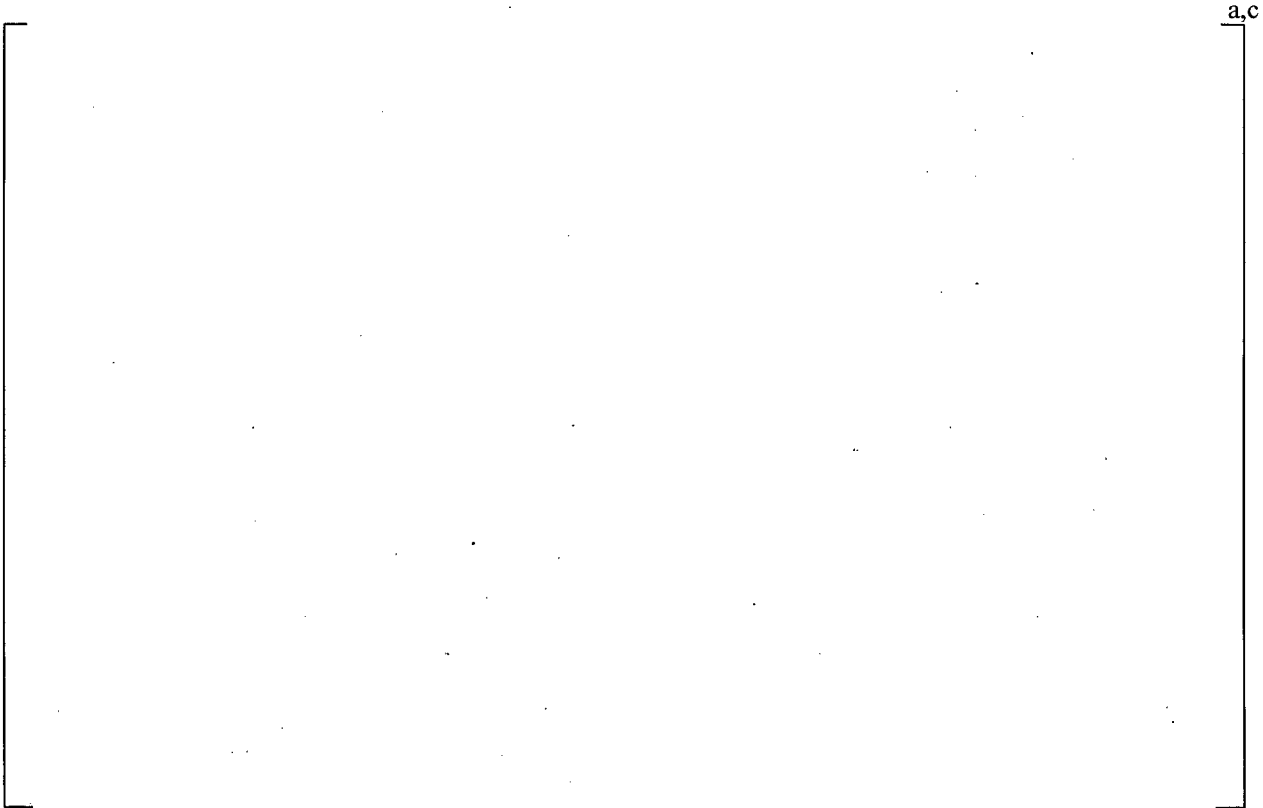


**Figure 8-23** |

]<sup>a,c</sup>

## 9 SUMMARY OF RESULTS AND CONCLUSIONS

[

] <sup>a,c</sup>

[

] <sup>a,c</sup>.

a.c

Table 9-1 Summary of Results: EPU Conditions	

**Table 9-2 Summary of Results: CLTP Conditions**

a.c

--

---

## 10 REFERENCES

1. Westinghouse Electric Sweden AB Report SES 09-127, Rev. 1, Monticello Steam Dryer Replacement – Structural Verification of Steam Dryer," June, 2010. (WESTINGHOUSE PROPRIETARY)
2. ASME Boiler and Pressure Vessel Code, 2004 Edition, Section III, Division 1.
3. ASME Boiler and Pressure Vessel Code, 2004 Edition, Section II, Part D.
4. U.S. Nuclear Regulatory Commission, Regulatory Guide 1.20, Rev. 3, "Comprehensive Vibration Assessment Program for Reactor Internals During Preoperational and Initial Startup Testing," March 2007.
5. Westinghouse WCAP-17252-P, Revision 0, "Acoustic Loads Definition for the Monticello Steam Dryer Replacement Project," June, 2010.
6. [ ]<sup>a,c</sup>.